Working Papers of the Finnish Forest Research Institute 297
http://www.metla.fi/julkaisut/workingpapers/2014/mwp297.htm
ISBN 978-951-40-2476-4 (PDF)
ISSN 1795-150X

A prediction model prototype for estimating optimal storage duration and sorting

Gernot Erber, Johanna Routa, Lars Wilhelmsson, Jyrki Raitila, Maunu Toiviainen, Juho Riekkinen and Lauri Sikanen

METLA www.metla.fi

Working Papers of the Finnish Forest Research Institute publishes preliminary research results and conference proceedings.

The papers published in the series are not peer-reviewed.

http://www.metla.fi/julkaisut/workingpapers/
ISSN 1795-150X

Office
Post Box 18
FI-01301 Vantaa, Finland
tel. +358 29532 2111
e-mail julkaisutoimitus@metla.fi

Publisher
Finnish Forest Research Institute
Post Box 18
FI-01301 Vantaa, Finland
tel. +358 29532 2111
e-mail info@metla.fi
http://www.metla.fi/

Authors

Gernot Erber, Johanna Routa, Lars Wilhelmsson, Jyrki Raitila, Maunu Toiviainen, Juho Riekkinen and Lauri Sikanen

Title

A prediction model prototype for estimating optimal storage duration and sorting

Year	Pages	ISBN	ISSN
2014	76	978-951-40-2476-4 (PDF)	1795-150X

Unit / Research programme / Projects

Joensuu Regional Unit / Forest Energy 2020/INFRES

Accepted by

Antti Asikainen, Professori, June 2014

Abstract

The objective of this study was to develop prototypes for estimating the optimal storage time and sorting of fuel wood. Drying trials employing the state of the art technology of load cell based metal frames were carried out by University of Natural Resources and Life Sciences (BOKU), METLA and Skogsforsk. A reference trial employing traditional pile sampling was carried out by VTT. Easily applicable drying models for logging residues, whole trees, stem wood and stumps were developed. A large variety of meteorological parameters can be used for model input. Parameters ranged from basic data like relative air humidity and air temperature to more complex parameters like evaporation and equilibrium moisture content of fuel wood. Fuel wood drying models can improve the fuel wood supply chain by helping the supplier find and choose those wood piles that are drier and thus with a higher calorific value for delivery. It enables supplier to deliver fuel wood which better meets the demands of the customers. Transport can be optimized by these models too. The drying models can also be used to formulate recommendations concerning seasoning of residues and optimum storage times for different assortment, species and drying conditions. An outlook on future application and further research needs was provided. Machine vision technology for sorting of fuel wood by quality and particle size, as well as for assessing the volume of a delivered fuel wood load was tested by VTT and JAMK. INFRES partners provided chip samples from all over Europe for testing. RGB images proved to work very well when identifying shapes and sizes of chips. If odd particles have the same colour as woody material, RGB images could not identify them. Measuring wood chip loads with a time-of-flight (TOF) camera rendered the most promising results. The average error was about 10%. Compared to visible light technology, near infrared (NIR) spectroscopy proved to be much more accurate in determining fuel wood moisture content and detecting foreign objects. Technology based on visible light is not able to work online (moving chips). To the contrary, NIR technology proved to work online and therefore could be used at a power plant or fuel wood terminal where wood chips are moved with a conveyer. However, NIR technology has other challenges such as not being able to give reliable moisture information with regard to frozen materials. Furthermore, an outlook on future research needs was provided.

Keywords

fuel wood drying, modelling, load cells, machine vision technology, near infrared spectroscopy

Available at

http://www.metla.fi/julkaisut/workingpapers/2014/mwp297.htm

Replaces

Aiemman julkaisun verkko-osoite. Poista tämä tekstirivi, jos sitä tarvita, mutta jätä kenttä.

Is replaced by

Uudemman julkaisun verkko-osoite. Poista tämä tekstirivi, jos sitä tarvita, mutta jätä kenttä.

Contact information

Johanna Routa, johanna.routa@metla.fi

Other information

The research of the INFRES project has received funding from the European Union Seventh Framework Programme (FP7/2012-2015] under grant agreement n°311881. The sole responsibility for the content of this flyer lies with the authors. It does not necessarily reflect the opinion of the European Communities. The European Commission is not responsible for any use that maybe made of the information contained therein.

Contents

1 Definitions 5

2 Part I: General concept of automated data recording for moisture content alteration estimation 5

2.1 Experimental background and target of the study 5

3 Storing of uncomminuted fuel wood for fuel wood supply chain improvement 6

3.1 Fuel Wood Storage 6
3.2 Fuel wood quality criteria and quality improvement through drying 8

4 General experimental design of automated data recording for moisture content alteration estimation 9

4.1 Load cell based frames 9
4.2 Meteorological stations 10
4.3 Further basic data and additional data from other sources 11
4.4 Material sample design and analysis 11
4.5 Challenges and possible drawbacks when carrying out automated data recording 13

5 Moisture content alteration modelling based on automated recorded data: Modelling and model validation 14

5.1 Possible modelling approaches 14
5.2 Modelling period length 15
5.3 Input data for modelling and possible data sources 15
5.4 Modelling: techniques, target and explanatory variables 16
5.5 Model validation 16

6 Case studies 16

6.1 Area description 16
6.2 Experimental design description 17
6.3 Modelling techniques and validation approaches employed for moisture content alteration estimation 22
6.4 Case study Austria: Results 24
6.5 Case study Finland A: Results 26
6.6 Case study Finland B: Results 29
6.7 Case study Sweden: Results 33

7 Fuel wood supply chain improvement through moisture content alteration models and possible application 38

8 Conclusions on the use of moisture content models for improving the fuel wood supply chain 40

9 Part II: Introduction to machine vision technology 42

10 Monitoring wood chip quality ... 42
10.1 Samples and testing equipment ... 42
10.2 Identifying wood chips ... 43
10.3 Determining moisture of wood chips ... 46
10.4 Determining the particle size of wood chips ... 47

11 Measuring the volume of a fuel wood load ... 50

12 Wood chip analysis using near-infrared spectroscopy ... 53
12.1 Moisture analysis using NIR ... 53
12.2 Characterization of wood chips using NIR ... 56
12.3 NIR instrumentation: chemical imaging and multipoint measurements ... 57
12.4 Artificial demonstration: detection of moisture differences in spray-wetted sample ... 59
12.4.1 The main measurement campaign ... 61
12.4.2 Invasiveness of the NIR-CI measurement: evaporation of moisture due to high-power illumination ... 64
12.5 Classification capabilities of NIR chemical imaging ... 67

13 NIR spectroscopy conclusions ... 70

14 Discussion ... 72

References ... 73

1 Definitions

Terms in this report are used according to the following definitions and descriptions:

- Forest fuel is primary stem wood, branches, bark, and included needles/leaves.
- Moisture content is the weight of water contained within or unseparated from the forest fuel as defined above, calculated as percentage of the total weight of the material (wet basis).
- Dry basis is the condition in which the solid biofuel is free from moisture.
- Dry matter is material after removal of moisture under specific conditions.
- Dry matter content is the proportion of dry matter in the total material on a mass basis.
- Stem wood originates exclusively from the trunk of a tree above the stump (bark, branches, stumps and needles/leaves removed).
- Logging residues are wood, bark and included needle/leaves which are separated during tree harvesting.
- Calorific value is the energy amount per unit mass or volume released on complete combustion.

2 Part I: General concept of automated data recording for moisture content alteration estimation

2.1 Experimental background and target of the study

The basic idea behind a series of continues scaling experiments of stockpiled primary forest fuels is to follow the drying and wetting processes caused by natural weather events. Frames under water absorbing control (e.g. metal) standing on load cells can be used for high precision continuous electronic scaling of piled loads representing different forest fuel materials. If experiments are carried out the traditional way, samples, either sample slices or sawdust, have to be taken from the pile from time to time. A major drawback is the inability to take samples from the material inside the pile without disturbing the pile structure. Furthermore, samples taken from the pile edges suffer from edge effects and do not necessarily represent the moisture content inside the pile (Neußer et al. 1981). Lastly, no continuous knowledge - only snapshots - on the drying behaviour of the pile can be gained.

Load cell based frames are a feasible option to bypass these issues. The metal frame holds the load, and the load cells supporting the frame continuously report the load weight. It can be assumed that any weight alteration of the fuel wood load is caused by moisture removal or wetting (if no material degradation or tare weight changes occur). If the moisture content of the load is assessed at the start of the continuous scaling, alterations in load weight can be translated into alterations in moisture content, and therefore the moisture content is known at any moment. For control purposes, samples will always have to be taken from the piles, either to assess dry matter loss effect or correct operation of the load cells.

A problem still unsolved – especially when studying drying of logging residues and whole trees are dry matter losses. These, like moisture content decrease, result in load weight decrease. Thus, samples have to be taken to distinguish between weight reductions caused by decay and drying. In the Swedish scaling experiments, small masses of wood have been used to reduce the cost of the frames. Based on calculations and observed tare weights of empty frames, the controlled effect of the minor changes in water content of these wooden parts were considered almost negligible in relation to the scaled weights of fuel load, variation in moisture content and load cell precisions.

Modelling moisture content alteration by meteorological data can be based on precise data gained from these load cell based frames.

The target of this study was to develop the basic experimental design for this type of experiment, and methods to develop moisture content alteration models based on this data. Gained knowledge should be presented thematically grouped. Experiment results should be displayed in their own chapter. Furthermore, an outlook on actual and possible future fields of application should be provided. In addition, a literature review on fuel wood storage and the most common quality parameters shall be provided.

Three studies have been carried out (in Austria by BOKU, in Finland A by Metla and in Sweden by Skogsforsk) employing this new technique. For comparison, one further study (in Finland B by VTT) is reported, carried out the traditional way.

3 Storing of uncomminuted fuel wood for fuel wood supply chain improvement

3.1 Fuel Wood Storage

Fuel wood is usually harvested throughout the year but mainly consumed in winter. It also requires seasoning in storage in order to lower its moisture. Fuel wood can be stored either comminuted (as chips or firewood) or uncomminuted (whole trees, stem wood and logging residues). Chips and logging residues can be affected by fungal growth and self-heating in storage piles, and therefore can suffer from fungal initiated dry matter losses. Dry matter losses are not likely to occur to that extent when storing fuel wood as stem wood (Jirjis 1995, Golser et al. 2005).

Uncomminuted fuel wood storage can be classified several ways. Firstly, it can be classified by the stored material type. Logging residues are often left at the harvesting site in small heaps for pre-drying (Nurmi 1999, Filbakk et al. 2011b). Usually after one summer they are forwarded to larger stacks for storage until or over the winter (Jirjis 1995). Other options are the immediate storage in stacks, or bundling of the logging residues and storage in stacks afterwards (Pettersson & Nordfjell 2007). Whole trees, especially from thinnings, are usually stored in stacks. Compaction and storing as bundles is possible too (Nordfjell & Liss 2000). Like whole trees, stem wood is stored in stacks as well (Nurmi 1999, Suadicani & Gamborg 1999, Golser et al. 2005, Filbakk et

al. 2011a, Gautam et al. 2012, Pari et al. 2013). To improve their drying performance, Golser et al. (2005) and Elber (2007) suggest both parallel and criss-cross storage of logs.

Under European conditions, the best drying rates can be accomplished in spring and summer (Nurmi 1995, Höldrich et al. 2006, Nurmi & Hillebrand 2007, Pettersson & Nordfjell 2007, Erber et al. 2012). The earlier wood is stored in the year, the faster it will dry to a specific point (Kofman and Kent, 2009) Due to the colder and wetter periods in autumn, fuel wood storage is affected by rewetting of the piles (Jirjis 1995, Nurmi 1995, Nurmi 1999, Elber 2007). Rewetting occurs at the end of winter too. Moisture from melting snow penetrates the piles (Nurmi & Hillebrand 2007, Pettersson & Nordfjell 2007). Throughout the year, rainfall can rewet the fuel wood piles and set back already achieved moisture content reduction (Kröll 1978, Elber 2007, Erber et al. 2012).

Favourable storing conditions for fuel wood are sunny, elevated and open, wind-accessible locations (Nurmi 1999, Nordfjell & Liss 2000, Golser et al. 2005, Elber 2007, Nurmi & Hillebrand 2007, Filbakk et al. 2011a). For logging residues pre-drying at the harvesting site is recommended (Jirjis 1995, Nurmi 1999). Defoliation at the harvesting site is beneficial both in terms of drying performance and nutrient cycle (Nurmi 1999, Suadicani & Gamborg 1999). Drying by convection in a stack is governed by air temperature, relative air humidity, wind speed and rainfall (Kröll 1978). According to Kofman and Kent (2009) wind access and solar radiation have the greatest impact on the drying performance. Logs mainly dry at the cut surfaces (Golser et al. 2005) and - to a lesser extent - through all openings in the bark surface (Nurmi & Lehtimäki 2010, Röser et al 2010). Later effect is further reduced by stacking of logs (Nurmi & Lehtimäki 2010).

Covering of piles, e.g. with a paper based cover is recommended, especially under wet conditions like in Scandinavia or Scotland for both logging residues and stem wood (Jirjis 1995, Nurmi & Hillebrand 2007, Pettersson & Nordfjell 2007, Röser et al. 2010, Filbakk et al. 2011a). No cover is necessary for stem wood under dry conditions like in Italy (Röser et al. 2010), but it probably could be beneficial in alpine regions too (Golser et al. 2005, Elber 2007, Erber et al. 2012). In the forest, covering of a pile is more important than in the open area, due to less wind access (Kofman &Kent 2009). Achievable effect of covering is considered to range from an additional 3– 6% reduction in moisture content compared to uncovered piles (Jirjis 1995, Nurmi and Hillebrand 2007). Jirjis (1995) reports a study where rewetting resulted in an increase of 20–50% in moisture content.

Dry matter losses during storage are an increasingly discussed topic. However, an accurate and convenient method for measuring dry matter losses from fuel wood storages has not been developed yet. In any case, several studies suggest dry matter losses that should be taken into consideration when fuel wood is stored. For logging residues, dry matter loss rates of 1–3% per month are reported (Jirjis 1995, Golser et al. 2005, Filbakk et al. 2011 b). Nurmi (1999) reports dry matter losses of 20% on the clear cut and 7% in the stack for the needles of logging residue during one year of storage. Pre-dried logging residues show lower dry matter losses (Filbakk et al. 2011b). Petterson & Nordfjell (2007) report a variety of studies, where drying rates of 2–12% for logging residues depending on the storage period and use of a cover were observed. At

their own experiments for compacted logging residues, dry matter losses of 9–18% were recorded during the storage period of 9–12 months. Pile heating and decomposition alike in chip piles are reported for logging residues piles (Golser et al. 2005). For stem wood, lower dry matter loss rates are reported. Golser et al. (2005) report less than 2% within the first year for most species. Higher

rates of up to 7% during the first year are reported for alder and poplar. After the first year of outdoor storage, decomposition speed of stem wood increases. For Pine stem wood a dry matter loss of 5% was recorded during an investigation period of 14 months (Erber et al. 2012). For fresh stem wood in Switzerland a dry matter loss rate of 1.8–4% per month is reported. Decomposition stops more or less when moisture content below 30% is reached (Elber 2007). Covering the piles can both increase the drying performance and reduce dry matter losses (Jiris & Lehtikangas 1993). Dry matter losses can be underestimated if the loss of volatile extractives other than water is neglected. Covering logging residues can result in up to 10% less moisture content compared to drying without cover (Jirjis 1995).

3.2 Fuel wood quality criteria and quality improvement through drying

During the last ten years, attempts have been made to standardize fuel wood quality criteria within Europe. These resulted in several European standards and standards in the draft phase.

European standards defining the properties and handling of solid biofuels (incomplete list; Austrian Standards 2014):

EN 14588 (Solid biofuels - Terminology, definitions and descriptions)
EN 14961 (Solid biofuels - Fuel specifications and classes) – 6 parts
EN 14780 (Solid biofuels - Sample preparation)
EN 15234 (Solid biofuels - Fuel quality assurance) – 6 parts

European standards in draft phase (incomplete list):

EN 17828 (Solid biofuels - Determination of bulk density)
EN 18134 (Solid biofuels - Determination of moisture content) – 3 parts
EN 18122 (Solid biofuels - Determination of ash content)
EN 18123 (Solid biofuels - Determination of the content of volatile matter)

In the following, the results of a literature review on the most common parameters, the calorific value and the moisture content is displayed.

One of the most common parameters in fuel wood quality assessment is the moisture content. It closely related to the calorific value, which increases with decreasing moisture content (Hartmann and Kaltschmidt 2001). Suadicani & Gamborg (1999) report a significant rise in calorific value for Norway spruce whole trees during one summer of drying. It is further related to the fines fraction - mainly needles and twigs. A ten percent decrease in moisture content results in a 26% increase in heating value (Elber 2007).

Drying fuel wood in piles by convection can help to decrease the moisture content significantly during one drying period. Drying can continue - to a lesser extent - during the next drying period (McMinn 1986, Stokes et al. 1987, Nurmi 1995, Pettersson & Nordfjell 2007, Gautam et al. 2012).

For Norway spruce logging residues, a moisture content drop from 56% to 28.5% (clear cut) and 42.2% (stack at landing) during one year of drying was observed by Nurmi (1999). Moisture

content of comminuted logging residues from the same clear cut had risen to 65.3% within nine months. Jiris and Lehtikangas (1993) stored Norway spruce logging residues for one year, starting in April 1990. In the covered part of the pile, moisture content decreased from 42% to 24–25%, whereas the moisture content in the uncovered part varied between 36% and 46%. By September the moisture content in the uncovered part had already dropped to 35% before rewetting occurred.

When drying pine and Norway spruce stem wood felled in spring moisture content dropped to 31%, whereas moisture content of alder and birch stem wood dropped to 37% (Hakkila 1962). Experiences from Austrian forest companies are reported in Golser et al. (2005). Broadleaf species stem wood dried 6–8 months during summer after harvest in winter. Final moisture content was 35–37%. After a period of 12–14 months a final moisture content of 29% could be achieved. When drying Norway spruce stem wood for 1–2 months, which was harvested in winter and largely debarked, the final moisture content was 25–35%. Erber et al. (2012) observed a moisture content decrease from 50.1% to 32.2% when drying a Scots pine stem wood pile for 14 months. Six Norway spruce and six beech stem wood piles in Switzerland dried from 45% (Norway spruce) and 38% (Beech) in moisture content to 41% (Norway spruce) and 34% (beech) during one year of storage. Final moisture content varied substantially (23–58% for Norway spruce and 31–37% for beech) between the piles depending on storing site and storing technique (Elber 2007). Nurmi & Hillebrand (2007) report a drop below 30% in moisture content during one summer under in-stand conditions for pine and birch stem wood and whole trees. Röser et al. (2010) tested the effect of debarking and covering stem wood at four experimental sites at Finland, Scotland and Italy. In Finland moisture content of the pine and alder logs dropped from 53% to 30% and 40% from April 2007 to February 2008. Sitka spruce dried at the Scottish trials in Glenlivet from 55% to 30% during the period of June 2007 to February 2008. Moisture content of Norway spruce and beech in Italy decreased from 50% to 30% (beech) and 43% to 28% (Norway spruce) from December 2007 to August 2008.

Nurmi (1995) reports a moisture content drop from 54 to 34% for willow whole trees from a short rotation plantation within 18 months of drying, starting in April 1992. Hakkila (1962) observed a better drying performance of Norway spruce, birch, pine and alder whole trees compared to drying stem wood.

4 General experimental design of automated data recording for moisture content alteration estimation

4.1 Load cell based frames

Metal frames, like the structure used on timber trucks, are used for holding the load. Frames are usually based on minimum four load cells, which allow permanent monitoring of the weight alteration of the load.

Expected load weight is up to 20 metric tons. Therefore, the load cells have to exceed this maximum load. Frames have to be placed on solid ground or reinforcement measures have to be

taken. For example, a second frame under the load cells, like in the Finland A experiment (Figure 1), can counter ground instability. Ground pressure can be distributed by putting metal plates or square edged logs under the load cells. It is vital to erect the frames free from distortive stresses to ensure precise load cell measurement.

Frames made from other materials, such as wood, can be affected more by air temperature and humidity than metal frames. If possible, the use of metal frames is the method of choice.

Load cells are linked to a data logger by cables or a wireless data transmission device. Data loggers can be used for recording data from the meteorological station too. Power supply is vital. Depending on the experiment location, either cable based or battery based power supply can be employed. Batteries need to be replaced from time to time or reloaded by solar power.

Data transmission can be specified by the type of location. If the experiment is set up at a research site, like in the Finland A experiment, both cable based and wireless short distance (WLAN) data transmission can be employed. Data transmission via GSM network is the method of choice for experiments far from research facilities. Another possibility would be a local storage of data. A drawback of this type of method is the inability to monitor pile weight permanently and the possibility of a long term undetected technical failure of the equipment.

Figure 1. Metal frame (left) and load cells (right) used at the Finland A experiment. Notice the supporting second frame below the load holding frame. Source: Metla.

4.2 Meteorological stations

Meteorological stations are needed to observed meteorological parameters at the study sites. Depending on the experiment location, either stationary or mobile types are used (Figure 2). Mobile types need independent power supply, by batteries, which are either replaced from time to time, or reloaded by solar power.

Depending on the experiment specification, different types of meteorological data are needed. Datasets usually contain data on relative air humidity [%], air temperature [°C], wind speed [m s^{-1}], wind direction [°], solar radiation [W m^{-2}] and rainfall [mm]. More sophisticated stations provide data on air pressure [hPa], ground temperature [°C], rainfall intensity [mm h^{-1}], and

Figure 2: Meteorological station types used for the drying trials. Mobile, solar powered type at Austrian trial (left), stationary at the Finland A trial (middle), and a simple but functional "€ 1000 station" in Sweden (right). Source: Gernot Erber, UEF and Lars Wilhelmsson.

visible distance [m], height of clouds [m] and snow depth [cm] too. A data logger collects all the meteorological data. Again, data transmission is depending on the experiment location and can be cable based, short distance wireless (WLAN) or wireless via the GSM network.

Air temperature and relative air humidity sensors can be placed in different pile layers. This is especially important when storing logging residues. Temperature rise inside the pile can lead to significant dry matter losses.

4.3 Further basic data and additional data from other sources

Pile volume of stem wood piles can be calculated from length and diameter measurements of each log. Volume of logging residue piles can be estimated by its dimensions. One has to keep in mind that density of the pile decreases from bottom to the top of the pile. Cut-to-length harvester production files (Arlinger et al. 2009) can be used to give a fairly detailed characterization of the amount and composition of forest residues (species, branches, tops, bark, needles/leaves), stem wood diameter, bark and species distributions (Möller et al. 2009). This can be a basis for predicting initial (fresh) moisture content as well.

Meteorological data alternatively or additionally can be gained from nearby meteorological stations or from meteorological data grids. Gridded data are produced using regional interpolation and generate estimates on the regional distribution of a weather parameter. Gridded data are commonly used in climate research.

4.4 Material sample design and analysis

Sample taking procedures are standardized in the EN 14780 and material type can be specified according to the EN 14961. Analysis of the moisture content, ash content and the volatile matter can be carried out as defined in the EN 18134, EN 18122 and EN 18123 (draft phases).

Moisture content at the start and at the end is important data for the experiments. If not only moisture content alteration but also actual moisture content should be monitored, starting moisture content is needed to have a starting value to start calculating from. Moisture content at the end is needed to verify the estimated moisture content.

Sample design differs between the assortments stem wood, logging residues and chips. Samples from all kinds of piles shall be taken from different height sections of the pile. Samples from the uppermost and lower section shall be avoided for edge effect reasons.

Samples from stem wood (Figure 3) can be taken as sample slices or as sawdust when cutting the logs with the chainsaw. The latter option involves possible contamination of the samples with chainsaw lubricants. Depending on the purpose, sample slices of different thickness can be taken up to 30 cm long sample sections. Samples slices shall not be taken from the edges of the logs to avoid edge effects. Only if samples are taken from the middle of the logs too, samples from the edges do not disturb the overall result. When taking samples by chainsaw, from experience a minimum distance of 50 cm from the log ends is necessary. An initial cut is necessary to open the log. Samples are then taken from the second, heartwood penetrating cut.

Samples from logging residues can be taken by chipping randomly chosen samples of logging residues. For this task, bigger amounts of material can be chipped and smaller subsamples can be taken from this amount. A garden chipper can be used for this. Chip moisture content then is assessed by the oven dry method. For fresh residues, even moisture content distribution can be assumed.

At the end of the experiments, either sample can be taken the same way as at the start, or the whole piles can be chipped and chip samples can be taken randomly.

Moisture content is assessed in a laboratory by the oven dry method according to current standards. Samples are weighed wet, then dried to the bone and then weighed again. The difference in weight is the share of water within the sample. Depending on the tree species, extractives can represent a small share of this weight. Needles and twigs hold more extractives than stem wood (Nurmi 1993).Wood density can be assessed after drying the sample slices to the bone based on the Archimedean principle. After sampling, material can be loaded into the frames by truck crane, forwarder or any other kind of crane.

Figure 3: Stem wood sample slices taken at the Austrian drying trials. Source: Gernot Erber.

4.5 Challenges and possible drawbacks when carrying out automated data recording

As with any kind of new technology and method, unexpected challenges arise during experiment set up and observation period. Apart from technical failure, several other problems may occur. In the following section, possible problems and actual problems from experience, as well as possible solutions shall be discussed.

To ensure correct dimension of frames, the expected load weight has to be calculated. Weak frames can deform and inflict stresses within the frames that can lead to inaccurate weight measurement. Load cells and frames need to be earthed to avoid load cell breakage from thunderstorms. Any other equipment like e.g. the meteorological stations needs earthing too (Figure 4).

Experimental design itself could possibly lead to overestimation of drying performance. Material is stored eventually higher above the ground than usual and the pile is possibly better accessible to wind. To counter this effect, the sides and the top can be covered by paper or similar cover. Another solution is building wooden wind walls (Figure 6) around the pile, only exposing the cross section to the wind as if the racks were part of a bigger pile.

Cables from the load cells to the data logger should be buried in the ground to avoid temperature effects on the load weight measurement. Furthermore, protection measures against rodents can prevent cables from getting bitten through. Burying cables in the ground can keep them from getting cut by accident (e.g. by machinery used) too (Figure 4).

Power supply is crucial for these experiments. Batteries can run out of power. When using solar cells for reloading, in periods of almost no sunshine battery voltage can drop below the point of possible reloading. Icy rain can cover the solar cells and limit their performance.

Apart from technical failure and breakage by storms, meteorological stations can suffer from the surrounding environment. Leaves can block the rain pitchers or algae can develop there.

Figure 4: Earthing of the frames to protect the load cells from lightning strike (left). Cables buried in the ground to prevent temperature effects on the measurement accuracy (middle). Metal net to protect the cables from rodent biting (right). Source: Gernot Erber.

Dry matter losses can have significant effects on the moisture content estimation precision. Especially when drying logging residues, estimated moisture based on mere weight monitoring can be significantly affected because of massive dry matter losses. Dry matter losses are caused by microbiological processes that biodegrade wood into volatiles such as carbon dioxide. The type of material, moisture, temperature, size and shape of the fuel wood pile, amount of nutrients, and oxygen content of the pile all together affect the microbial activity and degradation of fuel wood (Jirjis 1995, Nurmi 1999, Pettersson and Nordfjell 2007). Needles, leaves, and bark contain a large amount of living matter, water and nutrients, which accelerates mold and fungal growth. In suitable circumstances (moisture and temperature) microbiological activity could be vigorous.

Snow cover is another important issue. Firstly, snow cover affects total pile weight. Secondly, moisture originating from melting snow penetrates the piles in spring and wets the material. Then especially logging residues can suffer from increasing dry matter loss caused by increased fungal activity. Snow cover amount can be either measured by snow depth devices or estimated by calculation. Calculation bases on the assumption that, if pile weight increase and a temperature of below zero degrees are recorded, the rise in pile weight is caused by snow or ice. This rise in weight is divided by the surface area of the pile. Weight per m² then can be transferred into mm of rainfall.

5 Moisture content alteration modelling based on automated recorded data: Modelling and model validation

5.1 Possible modelling approaches

All approaches in fuel wood moisture content modelling have one common target variable: moisture contents or rather the moisture content alteration during a specified period. Alteration can be explained by a large variety of explanatory variables. These can be classified by their sources. Meteorological variables, like relative air humidity, air temperature, solar radiation, precipitation, reference evapotranspiration (Liang et al. 1996, Filbakk et al. 2011, Erber et al. 2012, Dong-Wook and Murphy 2013) and many more can be used for modelling. Parameters of storing, like the use of cover, the exposure and where a pile is situated (open land, edge of a forest, in the forest) (Filbakk et al. 2011) can be included. Material type (stem wood, logging residues, chips, firewood), state of processing (unsplit, split, chipped) and dimension (Stokes et al. 1987, Filbakk et. al. 2011, Dong-Wook and Murphy 2013), as well as, if there is no separated model for each, the tree species (Filbakk et. al. 2011) can have an influence. Duration of storage (Stokes et al. 1987, Filbakk et al. 2011) and season are possible variables.

Two major modelling approaches can be identified. Firstly, a more basic approach, that employs data as gained from meteorological stations and more than two variables. Secondly, a an approach that cumulates most of the data in the reference evapotranspiration and subtracts precipitation (Liang et al. 1996, Dong-Wook and Murphy 2013). Less common are approaches like as in Gigler et al. (2000), where drying of willow logs is modelled by employing a physical model based on different diffusivity coefficients of bark and wood. Simple drying models for stockpiled

roundwood and a practical tool for estimating drying rates per day and predicting critical drying when harvesting at different seasons in different parts of Sweden have been performed and published by Persson et al. 2003 and Wilhelmsson et al. 2004.

5.2 Modelling period length

When modelling fuel wood moisture content, different types of periods have to be taken into account.

First, the period of investigation has to be defined. Snow cover is an issue because of the missing knowledge about its decline and its rewetting the piles. In order to avoid this, drying models covering only the spring and summer period can be employed. Pile covers can be a reasonable measure to avoid melting snow penetrating the pile. Thus one can assume that snow at least does not have an effect on the moisture content. If snow weight is estimated by calculation, it can be subtracted from the pile weight. Snow weight can thus be kept out of the modelling process.

Second, depending on the intervals of data collection, the modelling time unit must be selected. Moisture content alteration can be calculated e.g. for 10 minute periods, hours, days or even longer periods like e.g. 10 day spans (Dong-Wook and Murphy 2013). Respective meteorological data needs to cover the same periods. Due to the fact that moisture content alteration is a rather slow process, short intervals in modelling do not work satisfyingly. It can be concluded from experience that modelling of moisture content on a daily basis is the shortest reasonable span of time.

5.3 Input data for modelling and possible data sources

Which data is needed for a model is often determined by the data available, not only for the modelling process itself, but also for the customer or user of the model. Any data needed for model application should be available without great difficulty.

Typical input for fuel wood drying models are meteorological parameters. Parameters such as air temperature, relative air humidity, solar radiation and precipitation are accessible almost everywhere. They can be measured by customary equipment at a reasonable price. If no meteorological station is available at the trial location, weather data can be gained either from nearby meteorological stations or weather grids. Weather grids allow interpolation of meteorological parameters for the specific location of the pile. They often offer a larger variety in data and e.g. potential evaporation can be gained from these grids too.

If important data is missing, it can be estimated by calculation. This is especially the case with any data concerning potential evapotranspiration. Allen et al. (1998) have listed a large variety of ways how to estimate this parameter and the parameters that are needed to calculate it. Subparameters, e.g. solar radiation can be gained from these formulas too.

5.4 Modelling: techniques, target and explanatory variables

For the process of modelling moisture content, different techniques can be employed. The most common way is the use of a linear or a multiple linear model. Mixed effect models, non- linear and polynomial approaches are also used frequently. Variance and residual analysis are basic parts of modelling procedure.

Target variables are limited to a small variety of variables that are closely related to moisture content. Moisture content alteration during a certain span of time is the most common target variable. Other possible variables are the reduction in weight in relation to the initial weight like in Stokes et al. (1987)

Since models are usually calculated separately for different tree species and assortments, explanatory variables mostly include meteorological parameters. Depending on the approach, either reference evapotranspiration and precipitation or air temperature, relative air humidity, solar radiation, precipitation, wind speed and wind direction are included.

5.5 Model validation

To verify fuel wood drying models, reference piles are one possible option. Samples must be taken from the piles, which should consist of similar material in assortment and tree species. Material should originate from the same cutting area and be stored like the material in the drying racks. Moisture content estimation is done by the model gained from the rack experiment. The result is compared to reference pile moisture content. The determination of the relative importance of a predictor variable is a key issue in the sensitivity analysis of fuel wood moisture content estimation model.

Model validation can be done by monitoring additional batches of desired biomass assortment and the changes from initial weight and in comparison with the changes in weight over time. Cross validation by data from the different experiments in different countries are also planned as a further development of the cooperative research.

6 Case studies

6.1 Area description

Four case study areas in three countries (Austria, Finland and Sweden; Figure 5) were selected for developing the prediction model prototype. Three of the experiments employed the state- of-the-art-technology of load cell based metal frames. One experiment was carried out the traditional way (repeated pile sampling).

AUSTRIA - Metal frames on load cells were located at a SMEs storing area (47°26’45.78”N, 16°20’19.80”E). Mean annual precipitation is 749 mm and mean annual temperature is 8.4 °C.

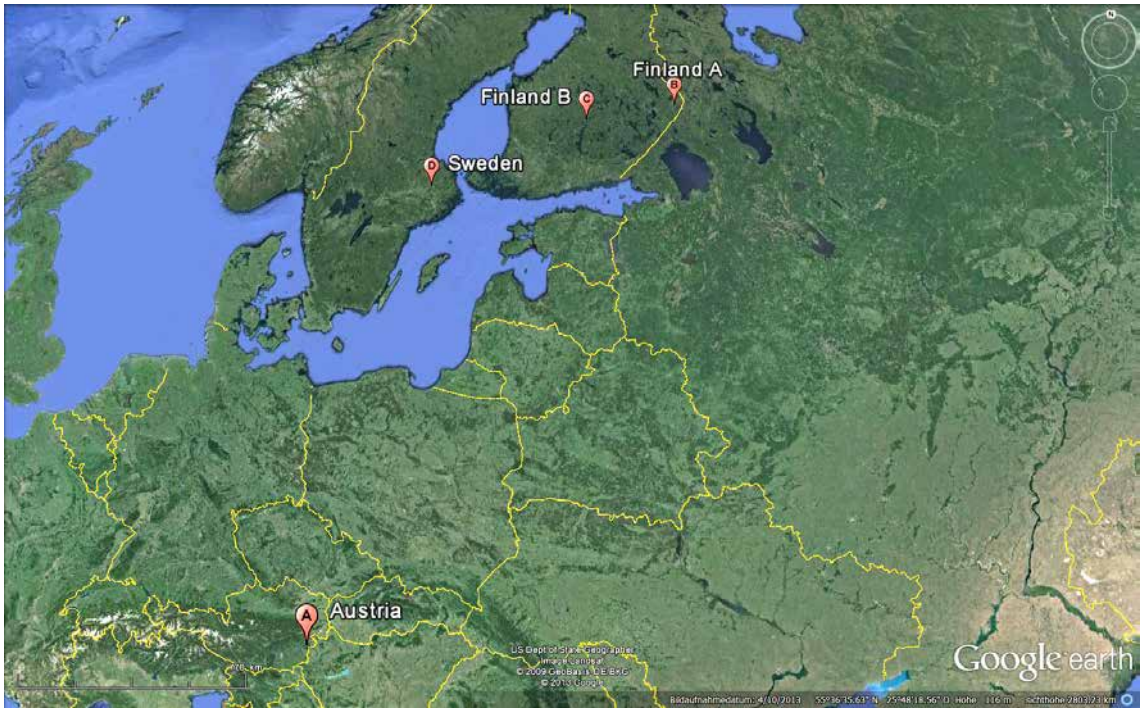

Figure 5. Location of the case study areas. Source: Google Earth.

The storage area is open, grassy land, elevated 371 m above sea level, slightly sloping to the east and skirted by a tree row in the south.

FINLAND A - At the Mekrijärvi Research Station of the University of Eastern Finland (62°46'N, 30°59'E), metal drying racks on load cells have been built for research purposes. Mean annual precipitation in this area is 668 mm and mean annual temperature 2.1 °C. The storage area at Mekrijärvi Research Station is an open area, next to a lake and its elevation is 155 m above sea level.

FINLAND B - several conventional piles were monitored in Central Finland within a radius of 50 km around Jyväskylä (62°14'N, 25°45'E).

SWEDEN - The test location, Strömsberg (60°14'N, 17°34'E, 20m above sea level) can be characterized as a well-drained flat land on a sandy soil close to a small river bank, not exposed to wind or other extreme weather conditions. It is rather a sunny than a shaded location. All weather information during May 2012 to May 2013 is given in 6.7 Results – Sweden.

6.2 Experimental design description

Five differently sized rack types (Table 1) were used in the experiments. Experiment Finland B was carried out the traditional way, employing periodically sampling of piles (Figure 8). Rack types in Austria and Finland were similar in size and shape (Figures 6 and 7), whereas two different types were used in Swedish (Figure 9) experiments. First, a double ship container rack was used for logging residue piles. Second, smaller wooden frames, holding small heaps of logging residues like the heaps on logging sites, were used.

Table 1. Specifications of the rack types used in the experiments: frame material, dimensions, load cell type and capacity and the number of frames.

Country	Frame material	Frame width × height × length [m]	Load cell type	Load cell capacity (kg)	Number of frames
Austria	metal	2.5 × 2.5 × 2.7	HBM RTN	4 × 15,000	1
Austria	metal	2.5 × 2.5 × 2.6	HBM RTN	4 × 15,000	1
Finland A	metal	2.5 × 2.8 × 2.6	Nokeval RMD 680	4 × 10,000	10
Sweden	metal	6.0 × 2.8 × 5.2	Vetek VZ266AS	6 × 10,000	2
Sweden	wood/resistant board	3.2 × 1.5 × 2.5	Scale beams WBV-1500	2 × 15,000	2

Figure 6. Austrian beech and oak stem wood drying trial 2013 (left) and beech stem wood drying trial 2014 (right) . Notice the wind wall in the picture on the right. Source: Gernot Erber.

Figure 7. Finland A stem wood and logging residue drying trials. Source: Metla.

Figure 8. Finland B stem wood drying trial pile. Source: Kari Hillebrand

Figure 9. Ship container (left and middle) and self-made wooden platform (right) drying trial types used in Sweden. Source: Lars Wilhelmsson.

Meteorological data (Table 2) was recorded by a stationary meteorological station in the Finland A and the Swedish experiments. Mobile meteorological stations were used in the Austrian and Finland B experiments.

Additionally, in the Finnish experiments, gridded data from the Finnish Meteorological Institute was used to calculate reference evapotranspiration (ET°) according to the universal standard of the FAO Penman-Monteith method (Allen et al. 1998). The grid used in Finnish climate studies in 10 x 10 kilometers wide.

In the Swedish experiment, reference evapotranspiration was calculated (ET°) according to the universal standard of the FAO Penman-Monteith method (Allen et al. 1998) from the meteorological data recorded.

In the Finnish A and Swedish logging residue experiments, sets of temperature sensors were placed inside the loads on the racks to measure temperature inside the pile. Swedish sensors measured relative humidity within the pile as well.

Table 2. Meteorological parameters recorded in the experiments.

Parameter	Unit	Austria	Finland A	Finland B	Sweden
relative air humidity	%	X	X	X	X
air pressure	hPa		X		X
air temperature	°C	X	X	X	X
ground temperature	°C		X		
wind speed	m s^{-1}	X	X	X	X
wind direction	°	X	X		X
solar radiation	W m^{-2}	X	X	X	X
rainfall	mm	X	X	X	X
rainfall intensity	mm h^{-1}		X		
snow depth	cm		X		
visible distance	m		X		
height of clouds	m		X		

Overall, a total of 31 pile drying cycles were observed (Table 3). Two drying cycles are still running in Austria. Logging residues were studied in 15, stem wood in 13 cycles. Whole trees were studied in two, stumps in one cycle. Species studied covered the typical species in the participating countries. Whereas European beech and sessile and English oak were studied in Austria, Scandinavian trials covered the species Norway spruce, Scots pine and downy birch. No covers were used in Austria. In Finland A experiment, covers were used for 11 of 17 pile drying cycles, in Finland B each of the six piles covered half. Two of the six piles in the Swedish experiments were covered.

Three different types of logging residues were used in the Finnish A drying trial. First green residues, directly from a clear cut, second, green residues pre-dried during winter at the clear cut and third, brown residues, which pre-dried at the experiment area in small heaps before loading them into the frames. Two different types of logging residues were used in the Swedish drying trial. First, green residues, directly from the cut and second, material from the same cut pre-dried during summer. In the Austrian experiment, stem wood (16 cm mean diameter, 4 m average length) was studied. Stem wood in the Finnish A experiment had similar dimensions (15 cm mean diameter, 4 m average length).

All load cell based piles were sampled at the beginning and at the end of the experiment. The Finland B piles were sampled on a monthly basis. Sample procedures and types are displayed in Table 4.

Table 3. Experiment specifications of the carried out drying experiments: tree species, drying period, drying cycles observed and use of cover.

Country	Tree species	Assortment	Drying period	Cycles	Cover use and type
Austria	European beech	fresh stem wood	02/2013–10/2013	1	no cover
Austria	Sessile oak & English oak	fresh stem wood	02/2013–10/2013	1	no cover
Austria	European beech	fresh stem wood	12/2013–running	2	no cover
Finland A	Norway spruce	logging residues	10/2011–06/2013	1	Covered 09/2012; Walki-cover
Finland A	Norway spruce	logging residues	04/2012–06/2013	1	no cover
Finland A	Scots pine	stem wood	04/2012–06/2013	2	one covered 09/2012; Walki-cover
Finland A	Norway spruce	logging residues	09/2012–06/2013	2	covered 11/2012; one Walki-cover, one JL-fabric
Finland A	birch	stem wood	11/2012–06/2013	2	covered 11/2012; one Walki-cover, one JL-fabric
Finland A	Norway spruce	logging residues	05/2013–06/2013	2	non covered
Finland A	Norway spruce & birch	stem wood	06/2013–02/2014	3	covered 06/2013; one Walki-cover, one JL-fabric, one not covered
Finland A	Norway spruce	logging residues	06/2013–02/2014	4	covered 06/2013; two Walki-cover, one JL-fabric, one not covered
Finland B	Norway spruce	fresh logging residues	04/2012–12/2012	1	partly
Finland B	Scots pine	fresh whole trees	04/2012–12/2012	1	partly
Finland B	broadleaf species	fresh whole trees	04/2012–12/2012	1	partly
Finland B	Scots pine	fresh stem wood	04/2012–12/2012	2	partly
Finland B	Norway spruce	fresh stumps	04/2012–12/2012	1	partly
Sweden	Norway Spruce, Scots pine	fresh logging residues	05/2012–05/2013	1	yes; net reinforced 4.0 m paperboard with pe-lamination; grammage of 246 gr m^{-2}
Sweden	Norway Spruce, Scots pine	fresh logging residues	05/2012–05/2013	1	no; small “harvester-made” stacks
Sweden	Norway Spruce, Scots pine	seasoned logging residues	08/2012–05/2013	1	yes; net reinforced 4.0 m paperboard with pe-lamination; grammage of 246 gr m^{-2}
Sweden	Norway spruce	fresh logging residues	07/2013–11/2013	1	no; small “harvester-made” stacks
Sweden	Norway spruce	fresh logging residues	11/2013–	1	no; small “harvester-made” stacks
Sweden	Norway spruce	fresh small diameter stem wood	11/2013 -	1	no; stem wood piles generally not covered

Table 4. Specifications of the samples taken at the experiments: material and sample type, sample amount and respective experiment stage.

Country	Material type	Sample type	Samples per pile	Experiment stage
Austria	stem wood	sample slices	35	start
Austria	stem wood	sample slices	24	end
Austria	stem wood	chip samples	10	end
Finland A	stem wood	sample slices	15-21	start
Finland A	stem wood	chip samples	3	end
Finland A	logging residues	chip samples	6	start
Finland A	logging residues	chip samples	3	end
Finland B	stem wood	sample sections	-	monthly
Finland B	whole tree	sample sections	-	monthly
Finland B	logging residues	sample sections	-	monthly
Sweden	logging residues	chip samples	6	start
Sweden	logging residues	chip samples	16	end
Sweden	logging residues	chip samples	6	start
Sweden	logging residues	chip samples	15	end

6.3 Modelling techniques and validation approaches employed for moisture content alteration estimation

At the Austrian trial, modelling was conducted two different ways. Before modelling, air temperature was converted from °C to K (Kelvin), to avoid ambiguous effects around temperatures of zero °C. Multiple linear regressions were used for parameter estimation. Firstly, the daily moisture content change (DMCday) should be explained by the mean daily air temperature, mean daily relative air humidity, mean daily solar radiation and mean daily wind speed, daily sum of precipitation and season.

DMCday = coef1 * air temperature [K] + coef2 * relative air humidity [%] + coef3 * solar radiation [MJ] + coef4 * wind speed [m s^{-1}] + coef5 * rainfall [mm] + coef6 * snowfall [mm] + coef7 * season

For the second approach, daily data had to be cumulated initially. Cumulated moisture content change (DMCperiod) should be explained in daily steps by the cumulated sums of mean daily air temperature, mean daily relative air humidity, mean daily solar radiation, mean daily wind speed and daily sum of precipitation.

DMCperiod = coef1 * air temperature [K] + coef2 * relative air humidity [%] + coef3 * solar radiation [MJ] + coef4 * wind speed [m s^{-1}] + coef5 * rainfall [mm] + coef6 * snowfall [mm] + coef7 * season

Model validation was carried out by residual analysis. Models will be improved by data gained in future. Thus models for either daily or periodically steps should be available.

At the Finland A trial, multiple linear regression models were used to model the daily moisture content alteration. The explaining variable was the net evaporation (calculated by subtracting the precipitation from the reference evapotranspiration, calculated according to the FAO- standard by Allen et al. (1998)).

At the Finland B trial, development of the moisture estimation model is based on a presupposition according to which changes in moisture of stored fuel wood depend on the type of fuel wood, initial moisture, ambient conditions of the storage and local weather. In order to define parameters of the model, moisture samples were taken regularly and local weather data were gathered.

Changes in moisture during a certain time period can be calculated with the following formula:

wi+1 = wi + a*ΣP/(wi- weq+b) + c*ΣE(wi- weq)

where

wi = water content of wood at time ti ($kgH_2O/kgdm$)

weq =water content at equilibrium depending on the relative air humidity and temperature

ΣE = evaporation during period ti – t(i+1), mm ΣP = precipitation during period ti – t(i+1), mm a, b and c are experimental coefficients

Coefficients a, b and c are derived from practical experiments so that the created function corresponds with moisture samples as well as possible. At the same, time coefficients a and c scale effects of precipitation and evaporation to the same level with changes in moisture of wood. For example, for pine stem wood these coefficients are a = 0.0028, b = 5, c = 0.0028. As more sampling data is gathered in the future, similar coefficients will be determined for other fuel wood types as well.

Calculation starts at ti=t0 and therefore w1=w0 is the initial moisture of wood. The time period ti t(i+1) can be for example a day, week, month or something else depending on how detailed information is available.

The Swedish modelling approaches were based on linear regression models where the dry substance of the fuel material at a given time or the change in moisture content over different time spans (e.g. day by day) is the response variable (dependent variable). The explanatory variables (independent variables) have all been extracted from simple weather station data. In addition to this, a drying potential variable was calculated as the difference between predicted current moisture content and moisture equilibrium (e.g. Simpson, 1998) according to a function extracted from the Hailwood-Horrobin equation (1946). As drying and inside wetting processes of wood material, especially when piled, are slow processes, a set of cumulated weather variables were tested in some of the model approaches. As drying and wetting processes at temperatures over and below the freezing point (~0°C) have to be separated, such components were included in the Swedish model approaches. Modelling the impact from snow is not simple, but nevertheless a potentially important component depending on winter conditions, pile coverage and possibilities of operational removal of snow. Pile/stack exposed area was also included in the model. Precipitation was regarded as snow when air temperature (1 m above ground) was below 0.5°C. The reduction of snow coverage was divided into a melting process (going into water) and a sublimation process of directly evaporating snow as a simple function of solar radiation. When measurements of snow coverage are included in common meteorological observations this can be used as an alternative to a weather based model. To get an accurate record of the initial moisture content and the species composition of the forest residue material, small diameter logs etc. standardized production files (StanForD 2010, Arlinger et al. 2012) from CTL-harvesters and biomass models have been used (Möller et al 2009). For all model development the possibilities for practical implementation

have been kept in mind. For this reason simple input of causal weather parameters and a balanced rigidity in response of the model have been focused.

6.4 Case study Austria: Results

During the first Austrian drying trial period from 01.02.2013 to 21.10.2013 moisture content of the piles decreased (Figure 10) from 43.5% to 22.5% (beech) and from 38.9% to 24.8% (oak). Mean air temperature during the drying period was 11.5 °C and mean relative air humidity was 77.7%. During the observation period, total rainfall of 530.9 mm was recorded and a total snowfall of 179.6 mm was estimated. Total solar radiation was 1943.7 MJ. Mean wind speed was 1.0 m s^{-1}.

Highest drying rates were recorded in April (-5.6% beech; -4.8% oak), June (-4.1%;-4.3%) and July (-5.2%; -4.3%). Due to rainy a May, the drying rate dropped to -0.9% for the beech pile. Rewetting took place at the oak pile (1.2%) and at both piles in September (1.4%; 1.8%). Dry matter losses were low (-0.7% beech; -2.4% oak) during the investigation period. Dry matter losses were determined by comparing initial and final bone dry density of sample slices from the same stems. Sample slices were taken from the fresh logs in the beginning and at the end of the experiment.

Two drying models were developed in Austria. The models shall be used for natural drying of beech and oak stem wood of four meters length and diameters of 9–25 cm for beech and 11–24 cm for oak. Application is recommended for the period of February till October. Notice that air temperature needs to be converted to Kelvin before applying the model formula. For the daily approach, the target variable is the moisture content alteration per day in% on wet basis. For the cumulated sum approach, the target variable is the moisture content alteration per period of accumulation (daily steps) in% on wet basis.

Sufficiently accurate models (Figure 11) could be developed by both approaches employed. The approach based on the daily input data resulted in a mean deviation of -0.32% ± 0.59% (beech, SE = 0.20; R^2adj = 0.63) / 0.02% ± 0.81% (oak; SE = 0.25; R^2adj = 0.71) of the models from the observed curves. The approach based on the cumulated input data resulted in a mean deviation of

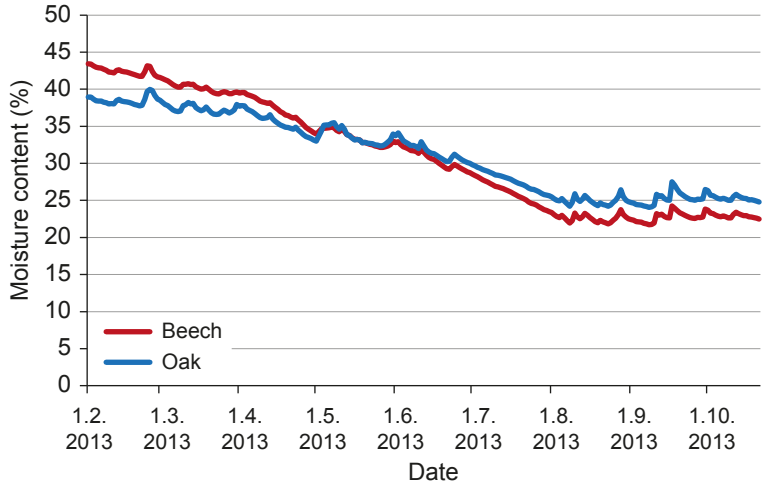

Figure 10. Moisture contents of the beech (red line) and oak (blue line) pile during the observation period in Austria.

-5.55 x 10–15% ± 0.74% (beech, SE = 0.74; R²adj = 0.99) / -1.27 x 10–14% ± 0.59% (oak; SE = 0.60; R²adj = 0.99) of the models from the observed curves. Daily moisture content alteration could be explained by the mean daily wind speed and the daily sums of solar radiation, rainfall, snowfall and by the season (Table 5). Cumulated moisture content alteration (Table 6) could be explained by cumulated sums of mean daily wind speed, air temperature, relative air humidity and the daily sums of solar radiation, rainfall and snowfall.

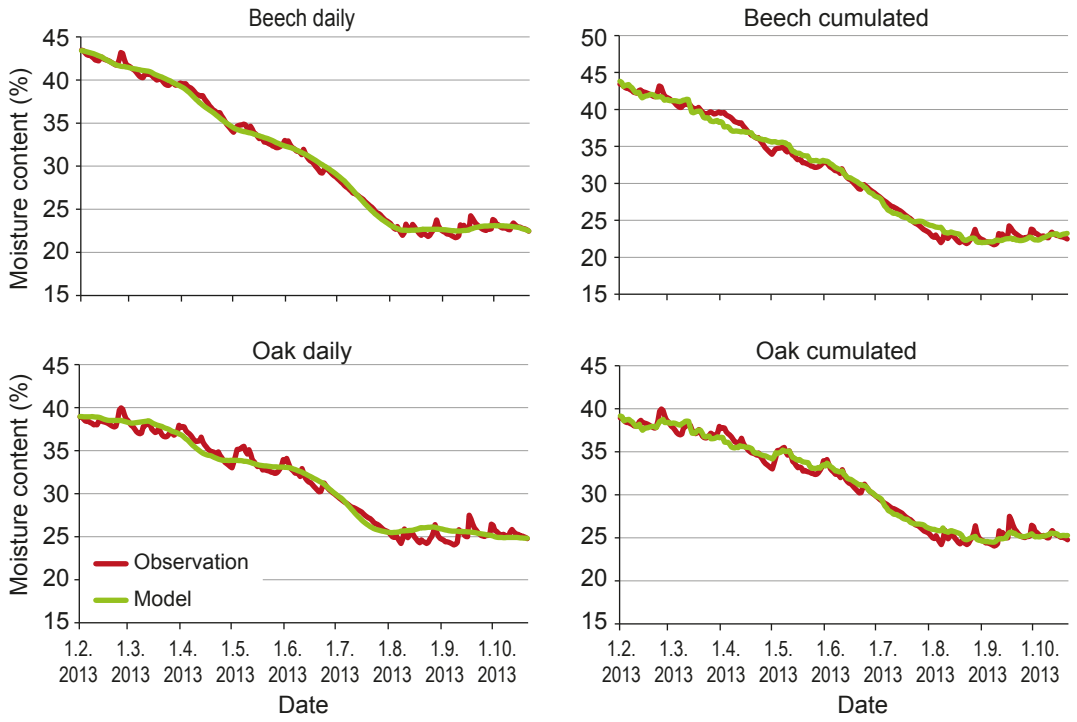

Figure 11. Observed (red line) and estimated (green line) drying curves of the beech (upper graphs) and oak (lower graphs) piles based on the daily (left) and cumulated (right) approach.

Table 5. Stem wood drying models (daily steps) for oak and beech in Austria.

Stem wood models based on daily means and sums for daily steps

DMC = coef1 * wind speed + coef2 *solar radiation + coef3 *rainfall + coef4*snowfall + coef5 * winter season

moisture content (i) = moisture content (i-1) + DMC

Model	Coef1	Coef2	Coef3	Coef4	Coef5	R² adj	SE
beech	-4.68×10^{-2}	-1.93×10^{-2}	4.54×10^{-2}	4.64×10^{-2}	1.65×10^{-1}	0.63	0.2
oak	-8.25×10^{-2}	-1.79×10^{-2}	7.24×10^{-2}	6.12×10^{-2}	-1.32×10^{-1}	0.71	0.25

Table 6. Stem wood drying models (periodical steps) for oak and beech in Austria.

Stem wood models based on cumulated daily means and sums for periods (p)

DMC = coef1 * wind speed [m s^{-1}] + coef2 *solar radiation [MJ] + coef3 *rainfall [mm] + coef4*snowfall [mm] + coef5*air temperature [K] + coef6*relative air humidity [%]

moisture content (i) = moisture content (i-p) + DMC(p)

Model	Coef1	Coef2	Coef3	Coef4	Coef5	Coef6	R² adj	SE
beech	-1.69×10^{-1}	-3.02×10^{-2}	-	-	-2.22×10^{-3}	-4.07×10^{-3}	0.63	0.2
oak	-1.13×10^{-1}	-2.37×10^{-2}	1.91×10^{2}	1.18×10^{-2}	1.84×10^{-3}	4.10×10^{-3}	0.71	0.25

6.5 Case study Finland A: Results

Significant differences were found in the drying curves between calculation methods with logging residues at the Finland A drying trial. A calculation method based only on the weight of logging residue piles in some cases underestimated the moisture content. Dry matter loss including methods achieved drying curves with the same final moisture content as assessed from samples by laboratory analysis (Figure 12). Some of the frames were unloaded in winter time, so there is a peak in the drying curve when the snow was removed from the pile before unloading. However, taking samples was very challenging. Moisture content within the pile varies and using the average moisture content of all samples doesn´t necessarily represents the real average. Range of variation in samples taken from the top, middle and bottom of the pile was remarkable. During the first drying period from different starting dates (15.11.2011, 13.4.2012 and 28.9.2012) to the unloading date (6.6.2013), the moisture content of logging residues decreased 8–10% and increased 4% in one pile. Highest drying rates were recorded in May 2012 (-6%), May 2013 (-11.5%). The first drying season (summer 2012) was very wet. Most of the precipitation was recorded in July (163.8 mm) and June (104 mm). A total of 557.4 mm during summer 2012 differed significantly from the long term average of 373 mm.

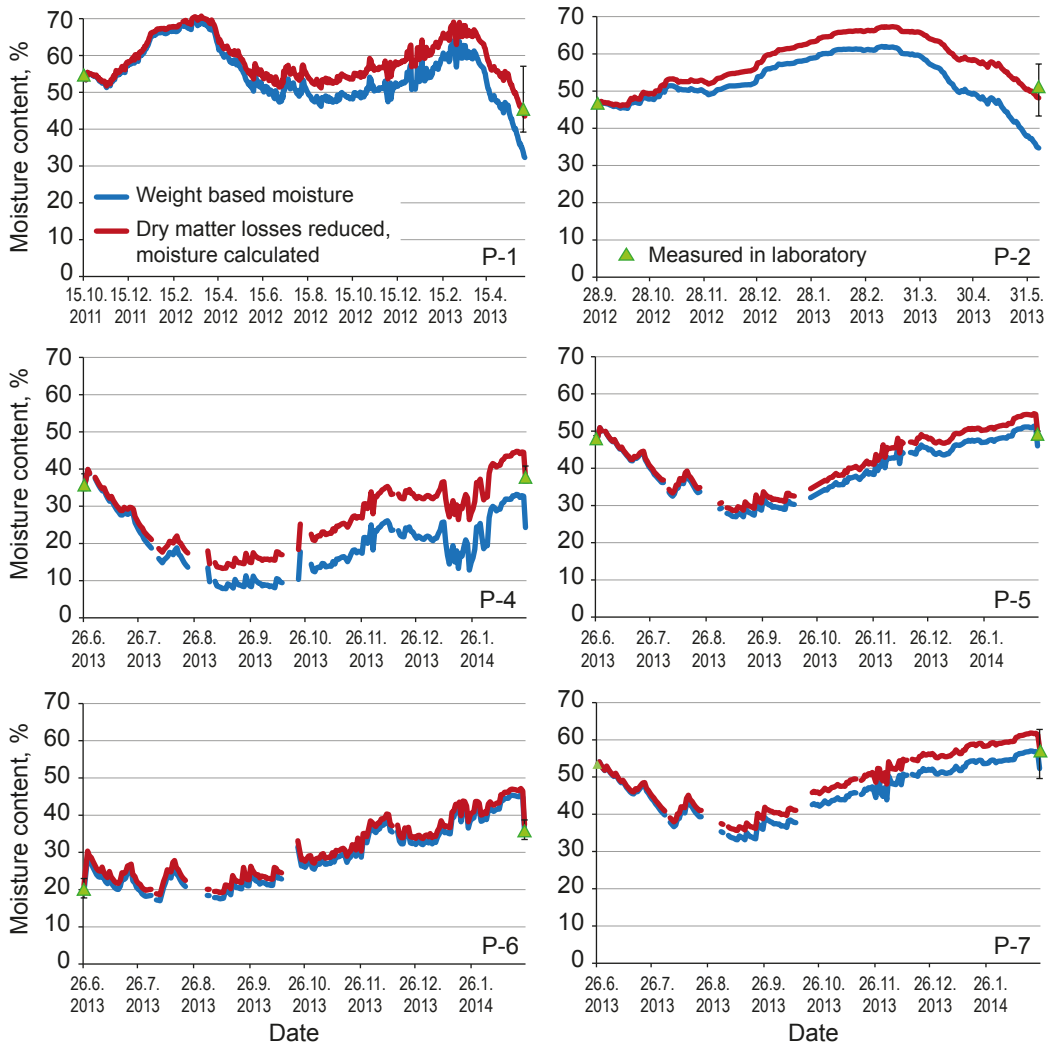

Figure 12. Observed drying curves of logging residues in Finland A experiment. Moisture content calculated based on weight and calculated with dry matter losses reduced. In addition, the real moisture in the end of the experiment was measured in a laboratory. The weight of snow is including in the weight, so it doesn't respond to the real moisture of the logging residues during winter months.

During the second period (26.6.2013–24.2.2014) moisture content of logging residues increased 1–4 percentage units. Brown residues pile's (starting moisture 20%) moisture content increased up to 15% during the storage period. Highest drying rates were recorded in July 2013 (-15%). Smaller piles and small heaps for pre-drying dried very effectively. Within six weeks, moisture content decreased from 46% to 19.3% and 20.8%.

The moisture content of small diameter stem wood (Figure 13) decreased during the first period (starting dates 29.3.2012 and 15.11.2012 to 6.6.2013) 13–23%. A decrease of 4–16% units was recorded during the second period (26.6.2013–24.2.2014). Highest drying rates were recorded in May 2012 (-6.5%) and July 2013 (-7.9%).

The models developed explain change in moisture content by net evaporation which is the difference between evaporation and precipitation.

DMCday = coef * net precipitation + const

Seven different drying models were developed in the Finland A trial. There are models for logging residues in roadside storage (covered and uncovered), small diameter stem wood in roadside

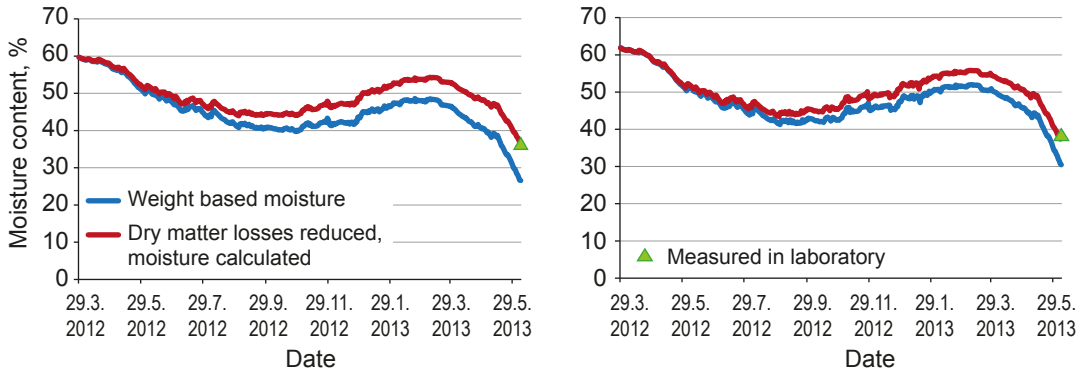

Figure 13. Observed drying curves of small diameter stem wood.

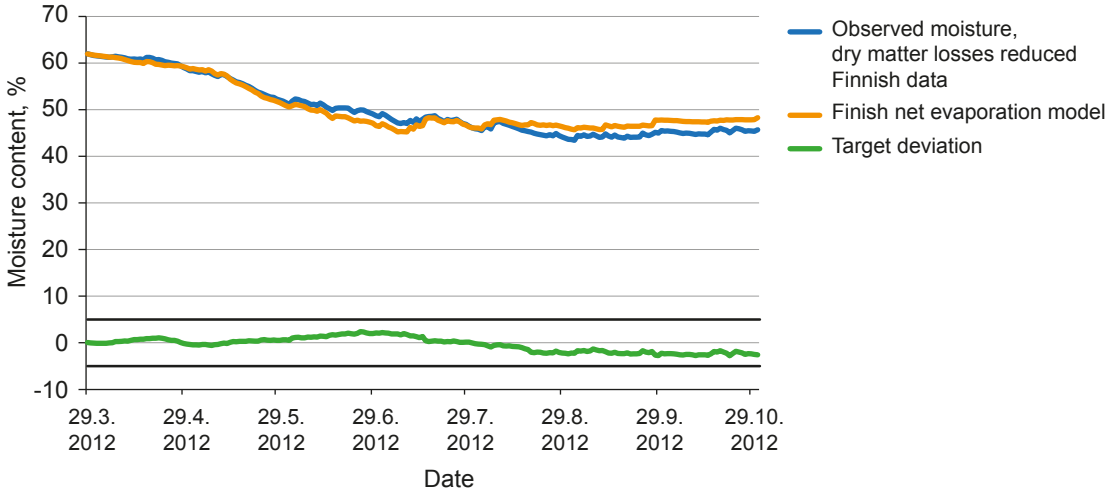

Figure 14. Observed (blue line) and estimated (orange line) drying curves of the pine.

storage (covered and uncovered). Furthermore, there are models for small heaps predrying in stands. Data for those models originated from the seasons spring, summer and autumn, so the moisture alteration during winter cannot be estimated by those models. Application therefore is recommended for the period of April to October. It can be assumed that the moisture content of energy wood increases in springtime, when melting snow penetrates the piles. For the daily approach, the target variable is the moisture content alteration per day in% on wet basis (DMC = daily moisture change). Stand models (Table 7) and roadside storage models (Table 8) were developed.

Using of the Finnish model starts with moisture content of fresh wood. For that reason, moisture content of fresh wood, depending of the cutting month, is presented in Table 9.

Table 7. Stand drying models for stem wood and logging residues in Finland.

Stand models				
DMC = coef * (evaporation – precipitation) + const				
moisture content (i) = moisture content (i-1) – DMC				
Model	**Coef**	**Const**	**R^2**	**SE**
stem wood	0.244	-0.1439	0.96	0.1
logging residues	0.246	-0.215	0.56	0.2

Table 8. Roadside storage drying models for covered and uncovered stem wood and logging residues in Finland.

Roadside storage models				
DMC = coef * (evaporation – precipitation) + const				
moisture content (i) = moisture content (i-1) – DMC				
Model	**Coef**	**Const**	**R^2**	**SE**
birch stem wood, covered	0.085	0.016	0.43	0.4
pine stem wood, covered	0.06	0.056	0.44	0.2
pine stem wood, uncovered	0.062	0.039	0.64	0.2
logging residues, covered	0.0776	-0.0472	0.59	0.4
logging residues, uncovered	0.163	-0.051	0.57	0.5

Table 9. Fresh moisture contents of stem wood and logging residues depending on the month of cutting in Finland.

Moisture content (%) of fresh stem wood depending on the month of cutting

Species	**Jan**	**Feb**	**Mar**	**Apr**	**May**	**June**	**July**	**Aug**	**Sep**	**Oct**	**Nov**	**Dec**
pine	57	57	57	56	56	55	55	57	57	57	57	57
spruce	57	57	57	56	56	55	55	57	57	57	57	57
birch	44	44	43	46	51	46	43	42	42	47	48	47

Moisture content (%) of fresh logging residues depending on the month of cutting

Species	**Jan**	**Feb**	**Mar**	**Apr**	**May**	**June**	**July**	**Aug**	**Sep**	**Oct**	**Nov**	**Dec**
pine	57	57	57	56	56	55	55	57	57	57	57	57
spruce	57	57	57	56	56	55	55	57	57	57	57	57
birch	44	44	43	46	51	46	43	42	42	47	48	47

6.6 Case study Finland B: Results

At the Finland B drying trial, whole tree piles' moisture content decreased from about 50% to below 35% during the period of May to December. Rewetting of about 5% took place in August. Both stacks dried equally well (Figure 15). Delimbed pine stems (Figure 16) dried differently, dependent on the use of a cover. Whereas the pile uncovered at the start hardly dried at all during summer, the pile covered from the start dried all summer. Starting from moisture contents of between 55–60% the moisture content decreased to about 35% (covered) and 45% (covered at the end of August). Logging residues (Figure 17) gained moisture in May and June. Finally, the same moisture content as at the start was reached after covering the pile in late August). Stumps dried much better, although no cover was used. Their moisture content dropped from about 55% in April to about 27% in September. After rewetting in autumn, the final moisture content in December was 37%.

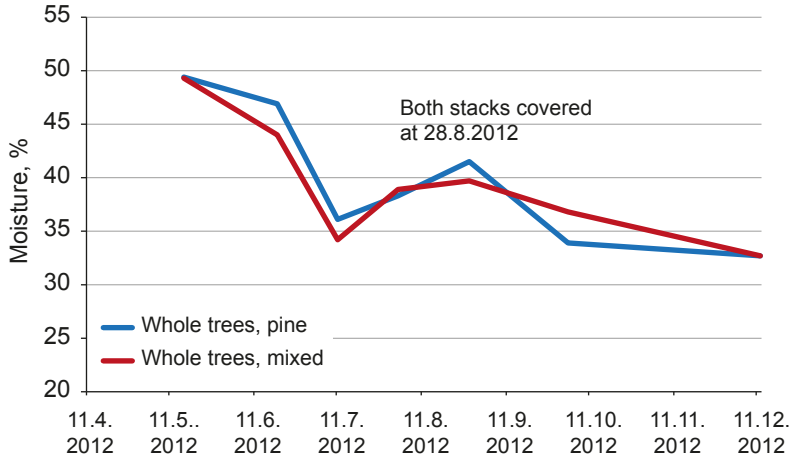

Figure 15. Observed drying curves of pine (orange line) and mixed species (blue line) whole tree stacks in Finland B experiment. Both piles were covered at the end of August to protect the stacks from rain and snow.

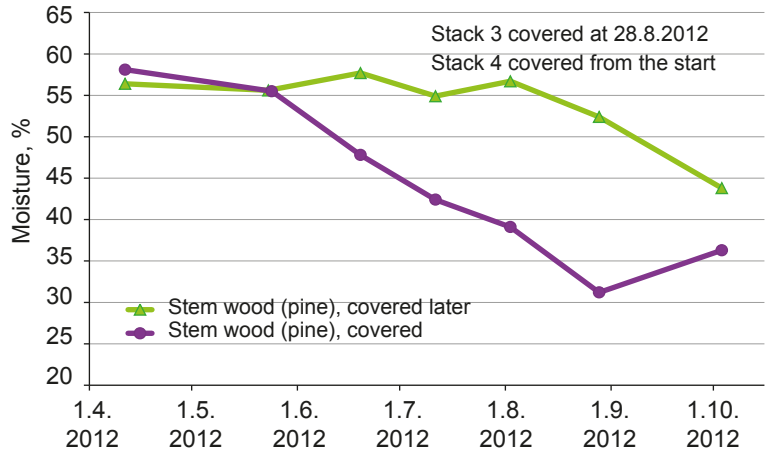

Figure 16. Observed drying curves of pine delimbed short wood stacks covered at the start (violet line) and covered at the end of August (green line). Due to heavy rainfall during summer, almost no drying occurred in the pile not covered.

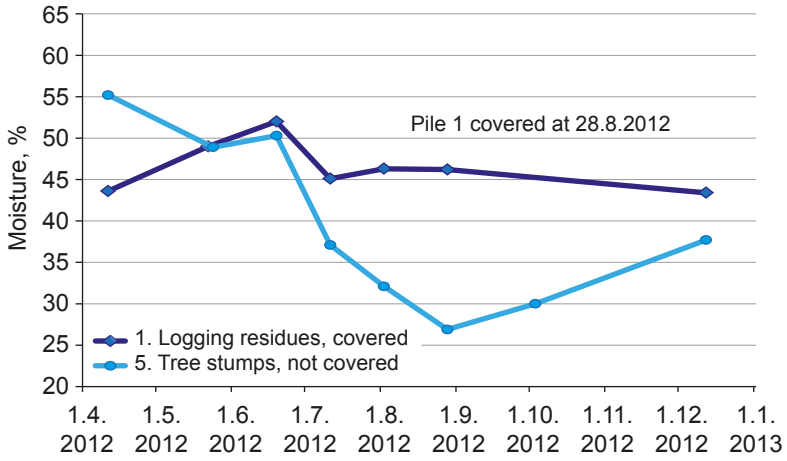

Figure 17. Observed drying curves of logging residues (dark blue line) covered at the end of August and tree stumps (light blue line). Drying performance of the logging residues was affected by rainfall.

The model developed explains change in moisture content by evaporation and precipitation sums. It is possible to estimate the moisture content for different lengths of periods, depending on the data available.

Different scenarios were calculated based on average long term weather data. The figures of average long term weather conditions gathered by the Finnish Meteorological Institute are presented in Table 10. The corresponding equilibrium moisture contents of fuel wood are calculated with a polynomial presented in Table 11. Similar polynomials can be derived from curves where measured equilibrium moisture contents are presented as a function of the air temperature and relative air humidity.

Drying performance was estimated for a delimbed pine stem wood fuel stack (coefficients used here were a = 0.0028, b = 5, c = 0.0028) for a period of two years, starting from different initial moisture contents. After two years, all stacks would have the same moisture content (Figure 18). If a cover is used to prevent a pile from rain and snow, an estimated gain in moisture content decrease of 5% compared to an uncovered pile can be achieved within one year (Figure 19).

Table 10. Average weather data 1991–2005 of the Finnish Meteorological Institute and corresponding equilibrium moisture contents.

Month	Precipitation (mm)	Evaporation (mm)	Relative air humidity (%)	Equilibrium moisture content of wood (%)
January	53	9	87	22.3
February	29	6	86	21.7
March	28	32	81	19.2
April	38	68	70	14.8
May	51	97	61	12.3
June	63	110	65	13.4
July	70	103	68	14.2
August	72	77	76	17
September	67	40	81	19.2
October	59	5	86	21.7
November	52	6	89	23.4
December	49	7	89	23.4

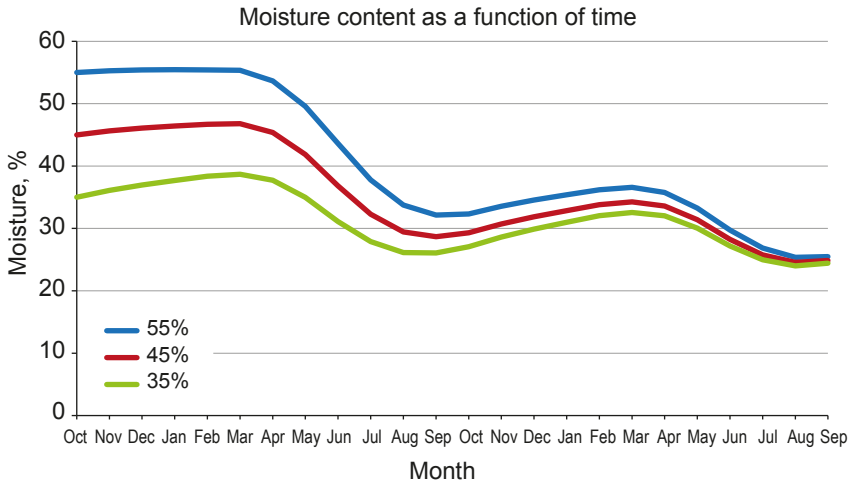

Figure 18. Moisture content estimated by the model based on long term average data for a delimbed pine stem wood fuel stack with different starting moisture content.

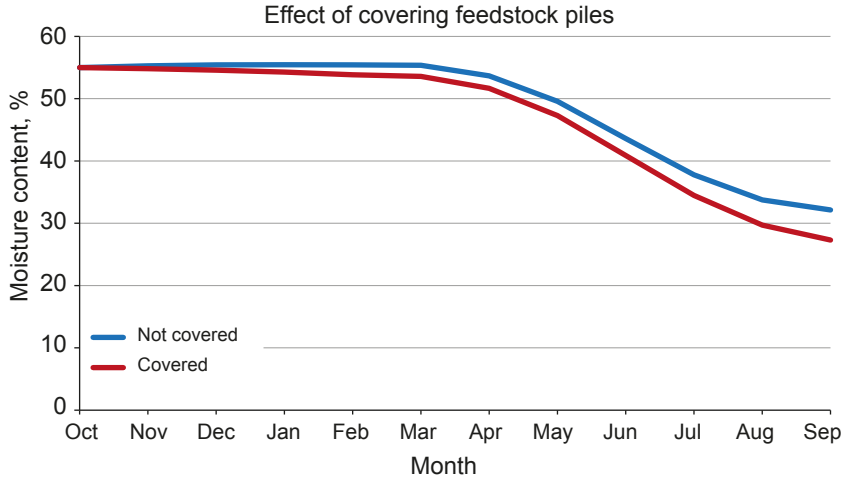

Figure 19. Moisture content estimated by the model based on long term average data for a fuel wood stack depending on if a cover was used (red line) or not (blue line).

Moisture content was estimated for a fuel wood stack (Figure 20). The first part of the recorded data was used for developing the model, whereas the second was used for verification. Two scenarios were calculated, which differed concerning the weather conditions in winter. It showed that the model estimated with satisfactory accuracy.

Average long term data can be used to calculate and predict changes of moisture in fuel wood. Parameters can be calculated on a monthly basis according to the formulas displayed in Table 11**.** Moisture content is then calculated as displayed in Table 12.

If evaporation is studied in detail, the surface temperature of fuel wood should be measured and the difference between the saturated air humidity and actual air humidity should be calculated. This remainder should then be scaled with a coefficient to correspond with actual evaporating moisture. This kind of measuring and calculating becomes quite complicated and time consuming, however. In addition, several other factors such as the size of wood logs, how they are stacked, the size of a wood stack and so on should be taken into consideration in order to increase the accuracy

of the model. In practice, many of these factors cannot be accurately known or measured, and therefore it is unnecessary to make the model too detailed.

In practical applications of the model, some of the most important other factors should be taken into consideration, however. One possibility is to add simple coefficients that describe the storage location and how the wood stack is made. For example, the height and the formation of the stack determine how much wood is exposed to direct rain. It is likely that high stacks remain drier on average because only the top layer gets wet when it rains.

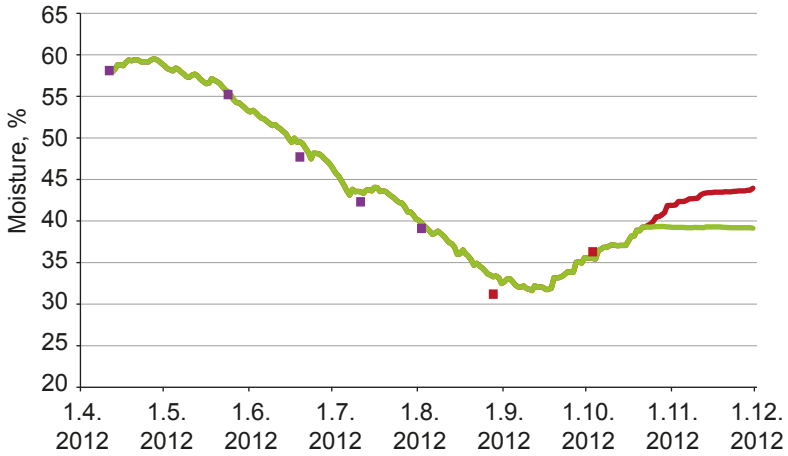

Figure 20. Moisture content estimated by the model based on data recorded during the period of April to August (violet squares). Model verification was carried out by samples taken later in the year (red squares). Different behaviour was estimated, depending on if the temperature in winter dropped below zero, (green line; all the precipitation is snow and wood is frozen) or not (red line; all the precipitation is rain).

Table 11. Parameter calculation for the Finland B drying model.

Parameter calculation on monthly basis

parameter = constant + coef1 * × +coef2 * x^2 + coef3 * x^3 + coef4 * x^4 + coef5 *x^5
with × = number of month (1: January – 12: December)

Parameter	Constant	Coef1	Coef2	Coef3	Coef4	Coef5	R^2
Equilibrium moisture content	6.00×10^{-2}	4.80×10^{-8}	-2.12×10^{-2}	6.00×10^{-4}	-7.00×10^{-6}	3.00×10^{-8}	
∑P	-70.15×10^{0}	126.47×10^{0}	-73.30×10^{0}	17.87×10^{0}	1.59×10^{0}	4.76×10^{-2}	0.99
∑E	128.38×10^{0}	177.15×10^{0}	-60.87×10^{0}	10.66×10^{0}	-7.76×10^{-1}	2.02×10^{-2}	0.99

Table 12. Finland B model for moisture content alteration calculation.

Moisture content calculation

$w_{i+1} = w_i + a*\Sigma P/(w_i - w_{eq}+b) + c*\Sigma E(w_i - w_{eq})$

w_i	water content of wood at time t_i [kg_{H_2O}/kg_{dm}]
w_{eq}	water content at equilibrium depending on the relative air humidity and temperature
ΣP	evaporation during period $t_i - t_{(i+1)}$ [mm]
ΣE	precipitation during period $t_i - t_{(i+1)}$ [mm]
a,b,c	experimental coefficients

6.7 Case study Sweden: Results

During the period 23.5.2012 to 22.5.2013, a total of 602 mm of precipitation fell, of which 71 mm fell at air temperatures below 0.5°C and was regarded as snow (65 mm at temperatures below 0 °C). Annual 24 hour average temperatures of 30 minute recordings from 0 °C and above (71% of the time) was + 9.9 °C and averages of all registrations below zero (29% of the time) was -5.5 °C. Relative humidity (24 hour averages) was 84% (minimum 25%) during temperatures above zero, and 88% (minimum 35%) during temperatures below zero. Recorded wind speed averaged 0.5 m/s (maximum 13 m/s) during plus degrees and 0.35 m/s (maximum 13 m/s) during minus degrees. Total solar radiation over the year was 882 kWh/m² of which 63 kWh/m² was recorded (slightly underestimated due to occasional snow cover on the solar integrator) during temperatures below zero. Maximum solar radiation was 970 W/m² during temperatures above zero and 637 W/m² during sunny winter conditions in March 2013 (causing snow sublimation).

The results showed generally good agreement between estimated and observed dry content including snow. Different expression of temperature, precipitation (rain and snow), relative humidity and solar radiation contributed significantly to explanation of changes in dry content. Including slower changing variables like 7 day averages of relative humidity, rainfall and solar radiation in combination with day by day averages resulted in flexible and somewhat rigid, not overreacting models. The maximum dry content was successfully controlled by a 21 day average of calculated equilibrium moisture content of the wood material. Figure 21 show the basic information needed to build the linear models.

The observed dry content was calculated as scaled changes in total weight in comparison with initial weight of dry substance and water respectively. Figure 22 shows the quick changes of total weight caused by snow coverage. Observe the relatively quick drying of all materials at the end of the drying period, when all snow melted. It indicates that the water from the melting snow coverage does not wet the residues to more than a limited degree. This is in line with earlier results

Figure 21. The models for estimating dry content of the logging residues were all built on explanatory variables extracted from a simple weather station.

and it also indicates that the residues under the snow coverage may be as dry as at the beginning of the winter season and that a successful removal of snow may be key to reducing high moisture contents in winter conditions deliveries of chipped residues. The differences between observed and estimated dry content varied between 1 and 6 percentage points for the larger piles (Figure 23 and 24) and between 1.5 and 3 percentage points of the smaller stacks (figure 25) over the modelled time span. The preliminary analysis of results from Tiny-Tags measuring temperature and moisture content in different positions inside the larger piles and the small stacks did not give evidence of any spectacular rises in temperature in any of the loads when compared with outside air temperatures.

Two models (Table 15 and 16) could be found for the Swedish piles, one for estimating the dry content of a fresh residue pile ($R^2 = 0.99$; SE= 2.5%) and one for estimating the dry content of small stack of residues ($R^2 = 0.99$; SE = 2.4%). Variable description and submodel calculation are presented in Tables 13 and 14.

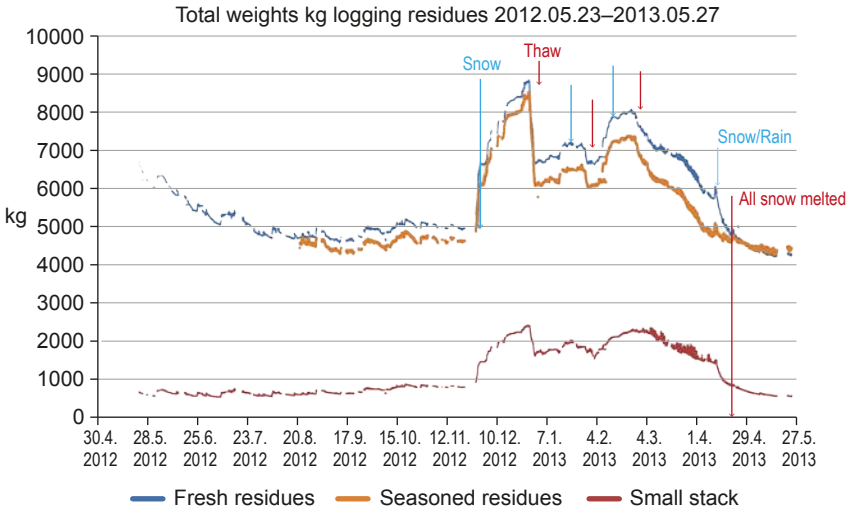

Figure 22. Overview of changes in total weights of larger piles with fresh (blue line) and seasoned (light brown) logging residues respectively and one of the small stacks (dark brown) simulating drying conditions at a harvesting object (seasoning). The impact of snow coverage is obvious. Observe that differences in weight of the small stack are shown at a comparatively low resolution.

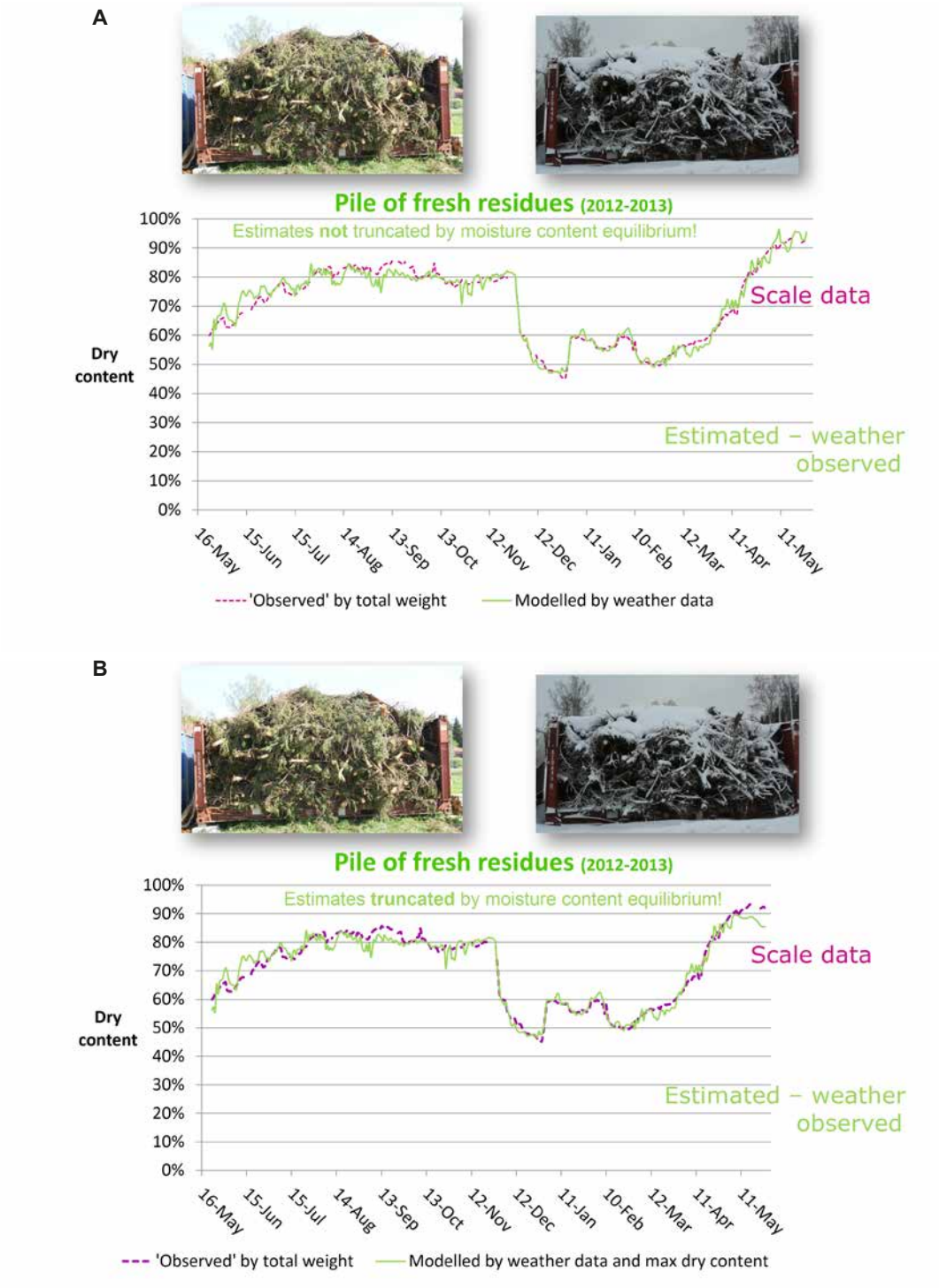

Figure 23. Above (A): Observed (by weight) versus estimated (modelled) dry content of logging residues, piled when almost fresh, i.e. 12 days after harvesting. The dip in dry content and quick recovery show the large effect of covering and melting snow which is included in all observed figures of the dry content. Below (B): Observed (by weight) versus estimated (modelled) dry content of logging residues, piled when almost fresh, i.e. 12 days after harvesting. Final weight according to the scale indicated a too high value of dry content. Here the model truncates the calculated value by the Equilibrium dry content according explained in table 13. Chip analyses show dry content between 84 and 86% at chipping by May 27, 2013 was in lines with the model calculation. The reason for the higher measured level can be underestimation of the initial MC which leads to general overestimations of dry content or mass losses. Some needles may have got lost, but there were no indications of mold attacks. The most likely explanation might be an overestimation of the start dry content.

Figure 24. Observed (scaled) versus estimated dry content of logging residues (by a level adjusted version of the model used for the fresh residues), piled and covered after seasoning in small stacks at the harvesting object for almost 100 days. As for the fresh residues, the dip in dry content and quick recovery show the large effect of covering and melting snow which is included in all observed figures of the dry content.

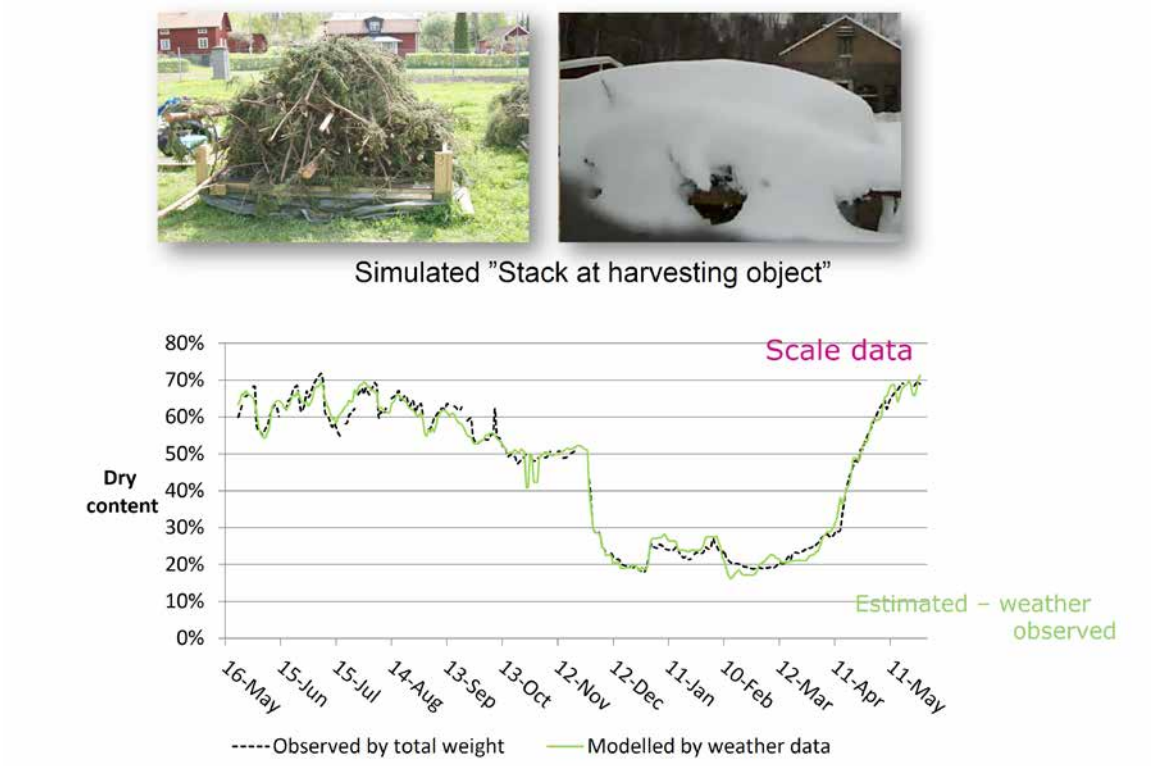

Figure 25. Observed (by weight) versus estimated dry content of a uncovered small stack of fresh logging residues designed to simulate the drying and wetting of uncovered seasoning stacks at the harvesting object. The large effect of snow and a somewhat smaller effect of melting can be seen in comparison with the larger and paper covered piles (figure 23 and 24).

Table 13. Weather variables and sub models used in the estimation models.

Variable	Unit	Explanation and submodels
variables controlling model phases		
SF	(0,1)	Non winter, 1 when no snow cover, 0 when snow cover
VF	(0,1)	Winter conditions, 1 when snow cover, 0 when no snow cover
S2	(0,1)	Season after winter, 1= when stored over winter (at the earliest February 1st) and no snow cover
INIMCD	%	Initial Moisture content at piling (calculated e.g. from harvester information, or from general experience or measured value at forwarding/piling etc.)
complex independent variables		
RHDry		RHDry=(100 RH)*((0.0002*(Airtemp**3))+(0.0114*(Airtemp**2))+-(0.3474*Airtemp)) if Airtemp<-0.5 then RHDry=0
Equilibrium dry content	% dry content	EquiMC=(-0.3467*(((RH7dy+RH21dy)/200)**3))+(0.41*(((RH7dy+-RH21dy)/200)**2))-0.2767*((RH7dy+RH21dy)/200)+0.9953 (Derived from the Hailwood-Horrobin equation and transformation to dry content.)
Drypot	% points	Drying potential defined as: Drypot=EquiMC-(1-INIFHD)
Snowacc	mm	See Precipitation variables in table below
other weather and time variables		
Accday	Days	Number of days from harvesting of the residues to the day estimated
RH1dy	%	Average Relative Humidity 24 hour backwards ≤100%
RH	%	Relative Humidity ≤100% (average per date)
RH7dy	%	Moving average of 7 days
RH21dy	%	Moving average of 21 days
Airtemp	°C	Temperature from weather station (average per date)
Airtemp1dy	°C	Temperature from weather station 24 hours backwards
Airtemp7dy	°C	Temperature from weather station 24 hours backwards
Solarrad	W m^{-2}	Solar radiation (average per day)
Solarrad7dy	W m^{-2}	Solar radiation, average per 7 days

Table 14. Precipitation, melting variables and submodels.

variable	unit	explanation and submodels
Precipitation	mm	Precipitation is rain or melted snow (heating unit) from the weather station
Snow	mm	If Airtemp<0.5 °C Precipitation counts as snow
Rainmm	mm	If Airtemp≥0.5 °C Precipitation counts as rain
Rainmm1dy	mm	Rain per 30 minutes during 24 hours backwards
Rainmm7dy	mm	Rain moving average per 30 min during 7 days backwards

Melt	mm	if ((Snowacc>0 AND Airtemp>0.1 AND Airtemp>0.1) OR (Snowacc>0 AND Airtemp>c)) then Melt=(a/Observationsperday)*((Airtemp-0.1)^1.2)
		if (Snowack>0 AND Rainmm>0) then Melt=Melt+(b*Rainmm*(Airtemp-0.1))
		where a=0.6 ; b=0.5 and c=4 for small stacks (Scale 3) and a=0.65 ; b=0.6 and c=2 for the larger pile (Scale 2).

Snowacc	mm	Snowacc=Snowacc+Snow-Melt, if snowacc<Snowacc+Snow-Melt then Snowacc=0;
Snowacc2		The pile was calculated to have a top surface of 6.1*5.2 m2 multiplied by Snowacc
Snowacc3		The stack was calculated to have a surface of 3.6*(2.5*1.5) m2 multiplied by Snowacc

Table 15. Model for estimating dry content in a pile of residues.

Residue pile model						
DryCont_Stack [%] = E1*a + E2 *b + SF * (E3 *c + E4 *d +E5 * f + E6 * g + E7 *h) + VF * (E8 * k + E9 * m) + S2 * (E10 * n + E11 * p + E12 * q + E12 *r + E13 * s) + e						
(a)	(b)	(c)	(d)	(f)	(g)	(h)
INIMCD2	Accdays2 * RH1dy	SF * Accdays2F * RHDry	SF * RHDry * Drypot	SF * Rainmm7dy	SF * RH	SF * Airtemp7dy
1.34×10^{0}	4.03×10^{-4}	1.24×10^{-4}	-1.49×10^{-3}	-3.59×10^{-1}	5.46×10^{-4}	3.43×10^{-3}
(k)	(m)	(n)	(p)	(q)	(r)	(s)
VF * Snowack2	VF * Solarrad7dy	S2 * Drypot2	S2 * Rainmm7dy	S2 * Airtemp7dy	S2 * RH7dy	S2 * RH21dy
-2.29×10^{-4}	1.80×10^{-4}	-7.97×10^{-1}	-1.30×10^{0}	2.13×10^{-2}	-5.30×10^{-3}	8.22×10^{-3}

Table 16. Model for estimating dry content in small residue stack.

Small residue stack model						
DryCont_Stack = E1 *a + E2 * b + SF * (E3 * c + E4 * d + E5 * f + E6 * g) + VF * (E7 * h + E8 * k) + S2 * (E9 * m + E10 * n + E11 * p + E12 * q) + e						
(a)	(b)	(c)	(d)	(f)	(g)	(h)
INIMCD3	Rainmm7dy * Accday * RH1dy	SF * Accday * RHDry	SF * Solarrad7dy	SF * Airtemp 7dy	SF * RH	VF * Snowacc3
1.05×10^{0}	-6.27×10^{-2}	2.31×10^{-5}	3.54×10^{-4}	5.79×10^{-4}	6.45×10^{-3}	-4.58×10^{-4}
(k)	(m)	(n)	(p)	(q)		
VF * Solarrad7dy	S2 * Drypot	S2 * Airtemp7dy	S2 * Solarrad7dy	S2 * RH21dy		
-9.12×10^{-5}	-1.66×10^{-0}	2.01×10^{-2}	1.48×10^{-3}	2.35×10^{-3}		

7 Fuel wood supply chain improvement through moisture content alteration models and possible application

Moisture content estimation models can improve the fuel wood supply chain by knowledge on where which wood stack is ready for chipping according to the specifications of the customer.

A fuel wood management tool would need several types of information to provide individual moisture content for the stored wood stacks:

Information about the pile is needed to localize it and to know which type of material is stored.

- Pile ID (identification which is unique for the pile; if there are more piles at a location piles eventually could be marked)
- Location of the pile (coordinates, eventually description)

- Date of storing
- Pile volume (estimated, e.g. from harvester data)
- Species (coniferous, deciduous or per species and share in percent, e.g. from harvester data)
- Assortment (logging residues, stem wood, whole trees, other)
- Processing and storing (splitting, use of cover)
- Initial moisture content (could be found from either samples or tables on the average fresh moisture content per species and month of the year)

Depending on this information, the appropriate model and model parameters are chosen for the pile.

Then, meteorological data is put into the model. In order to make moisture content estimation user friendly, meteorological data should be easily acquired and automatically fed into the fuel wood storage tool. Depending on the model, different data can be required.

- air temperature (°C)
- relative air humidity (%)
- wind speed (m s^{-1})
- solar radiation (MJ)
- potential evapotranspiration [mm]
- rainfall (mm)
- snowfall (mm)

Meteorological data can be either taken from the nearest meteorological station or from weather grids provided by the national meteorological organizations. If no real-time meteorological data is available, long term averages can be used. If the end user has his own stations available, these could be used as well.

The user must specify the desired material type and moisture content range.

Moisture content is then estimated by the chosen model based on the meteorological data periodically. If a pile nears the desired moisture content range, the user gets an alarm message. He can then decide if he wants to chip the pile immediately or not. Date of chipping can be specified and another alarm will be sent if the pile exits the desired range due to bad weather conditions. The user then can delay the chipping date. Moisture content can not only be estimated but also a pre-estimated by weather forecast. Automatized data input again would help to ensure user friendliness. Process flow diagram of a possible fuel wood management system is displayed in Figure 26.

Calorific value could be calculated based on moisture content estimation. Furthermore, dry matter losses could be included into the model. This could be achieved by storing time related dry matter loss tables.

The fuel wood management tool could be combined with or included into a GIS application, which would allow routing to the piles and an overview of the pile distribution.

Model performance could be improved by the pile's moisture contents which are assessed at the customer location (e.g. power plant) and the meteorological data used for estimating.

Another possible application would be a GIS-tool, which could be used for assessing suitability of an area for fuel wood storage. Long term average weather data, either from meteorological stations or weather grids, could be used in combination with other layers like e.g. land use (forest, open land) and road maps to detect areas best suitable both in terms of drying performance and logistics.

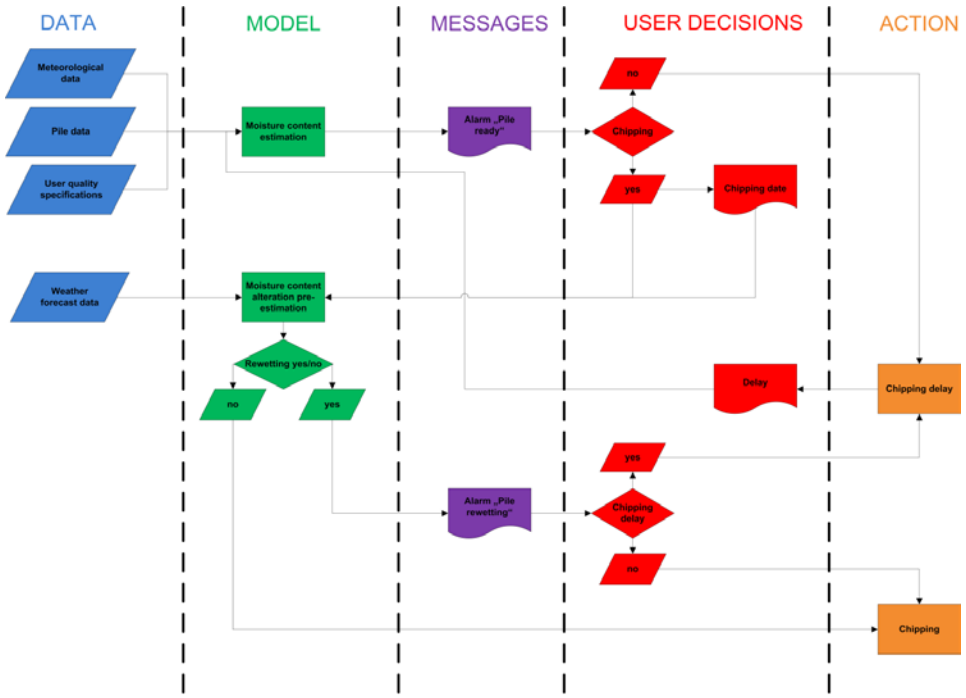

Figure 26. Potential process flow diagram of a fuel wood management tool.

8 Conclusions on the use of moisture content models for improving the fuel wood supply chain

Using load cell based automated data recording for fuel wood moisture content alteration estimation proved to be a feasible option to gain data for fuel wood drying models. Drying performance data has never been recorded in such a detailed manner before.

The modelling work compiled in this report show that it is possible to derive statistical linear models based on causal weather variables and specifications of wood material (type of material, initial moisture content and freshness). Weather conditions below the freezing point including snow coverage have to be separated from conditions above the freezing point including drying and wetting by rainfall. The implications of snow coverage can be different strongly depending on the pile volume in relation to the volume of covering snow. In addition, microclimatic conditions in the storage location affect drying performance remarkably. When using these drying models, this has to be taken into account.

Dry matter losses (caused by microbial activity, most commonly fungal attacks) can be a very important issue, especially when storing whole trees and logging residues. Self-heating of logging residues and whole tree stacks can inflict significant dry matter losses. Drying models need to incorporate these effects. Otherwise drying performance is overestimated. Dry matter loss rate per month could be taken from tables such as the table for fresh cut moisture content in the Finland A experiment.

Moisture content models could improve the whole fuel supply chain by helping the supplier find and choose those wood stacks that are drier and thus have a higher calorific value for delivery. Also, different boilers require different types of fuel. All in all, this kind of multivariate drying model would help optimize deliveries of fuel wood and therefore increase the efficiency of the whole fuel wood supply chain. In order to make this moisture calculating even more user friendly, all data should be easily and automatically acquired and fed into a suitable fuel wood management system, preferably integrated into an existing fuel procurement database.

Moisture content of wood material for energy isn't only the most important quality parameter for the customers but also of large importance for transport operations. Reports from practical flow of logging residues indicate large differences in observed moisture content at delivery (15–70% according to regular sampling). As different customers may prefer/accept different levels of moisture content there is a need for tools making it possible to estimate and measure the moisture content of stockpiled residues and stem wood at roadside. To start with the best possible accuracy of the initial moisture, content estimates could be made by biomass models operating on standardized cut-to-length harvester production files. Then changes in the average moisture of each fuel wood type can be estimated with the model and desirable logistical operations can be conducted based on these estimates.

The drying models can be also be used to formulate recommendations concerning seasoning of residues at harvesting objects, optimal storage time for fresh versus seasoned residues and stem wood depending on time of harvesting normal, best or worst case weather conditions, different kind of wood materials e.g. species, branches, tops, small or large diameter stem wood, effects of different piling principles, pile geometry, etc.

Some important questions and tasks remaining for further research:

1. Are the different models stable when estimating and predicting effects on different or varying weather conditions?
2. What are the consequences of using weather data from more remote weather stations or modelled grids in comparison with the high quality experimental setups?
3. How to predict and preferably avoid problems with mold and decomposition?
4. System analysis of value chain economy when including cost and benefits along the full chain from harvesting to energy supply from the power plant.

9 Part II: Introduction to machine vision technology

While the use of wood fuels, fuel wood chips in particular, is constantly increasing in Europe, a need to monitor quality and systematize sampling methods has become more common. New automated or semi-automated measuring methods and technologies are needed for measuring and monitoring wood chip quality more efficiently.

Machine vision technology is widely used in many industrial processes. Camera technology is constantly developing, yet prices of suitable cameras are quite moderate. Such cameras are easy to install in places where wood chips are delivered or they can be installed even on vehicles such as chip trucks. VTT has collaborated with Jyväskylä University of Applied Sciences (JAMK) in wood chip quality related projects before. Because they have excellent laboratory facilities and good experience from conducting machine vision testing, they were chosen to participate in this testing. After several planning meetings, it was decided that machine vision testing would be done in two phases. First, monitoring of wood chip quality was done in JAMK's laboratory in the spring of 2013, and then monitoring and estimating volumes of chip loads was performed at VTT in the summer of 2013.

Because machine vision utilizing RGB colour tone differentiation faces challenges in being able to determine moisture of wood, it was decided to conduct NIR spectroscopy testing as well. This was done at VTT's laboratory in Kuopio in the fall of 2013. The main goals of these tests and the study was to determine how machine vision technology could be used in monitoring fuel wood quality and measuring volumes of wood chip loads, and to understand limitations of the state-of-the-art technology in order to suggest further steps in practical application development.

10 Monitoring wood chip quality

10.1 Samples and testing equipment

Machine vision tests based on RGB colour tone differentiation to monitor quality of wood chips were conducted in the machine vision laboratory of JAMK. Several INFRES consortium members sent wood chip samples to be photographed with cameras and to be analysed for properties in an accredited biomass fuel laboratory (ENAS). The following samples were analysed:

VTT delivered wood chip samples in plastic bags to JAMK where smaller samples were taken from each bag and were put into a test rig tray for photography. It was possible to take pictures from different angles, to use different backdrop lighting and to take pictures of a moving sample when the tray was being slid onto the test rig. JAMK's test rig consisted of the following equipment:

- Servo controlled measuring station, able to move the camera, lights and sample tray
- Imperx colour machine vision camera
- LED matrix and fluorescent lamp for lighting
- PC operated control unit with National Instruments Vision Assistant and LabVIEW programs

Table 17. Wood chip samples that were with machine vision technology.

Sample	Moisture (%)
Boku1 (stem wood chips), Austria	30
Boku2 (stem wood chips), Austria	45
CTFC1 (stem wood chips), Spain	30
CTFC2 (stem wood chips), Spain	5
Ivalsa1 (stem wood chips), Italy	36
Ivalsa2 (stem wood chips), Italy	40
Freiburg1 (stem wood chips), Germany	<15
Freiburg2 (stem wood chips), Germany	>30
FinRankahake1 (stem wood chips), Finland	31
FinRankahake2 (stem wood chips), Finland	41
FinRankahake3 (stem wood chips), Finland	49
FinHakkuutähdehake (logging residues), Finland	49

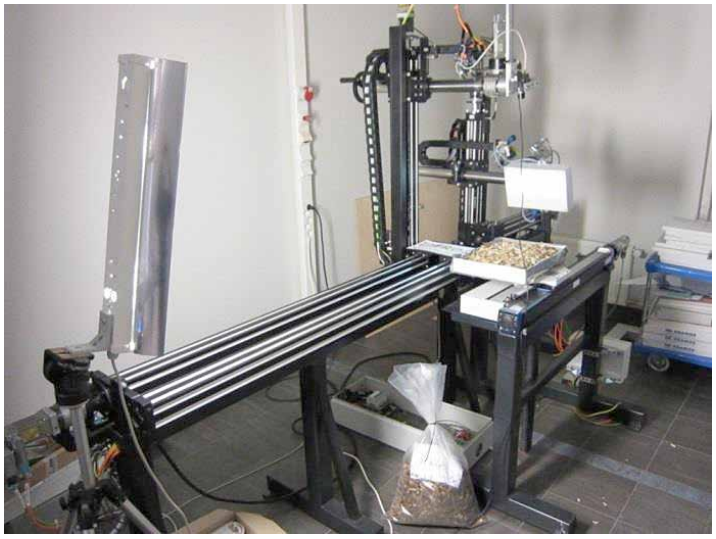

Figure 27. JAMK's machine vision test rig. Source: Juho Riekkinen.

10.2 Identifying wood chips

According to a test plan, eight pictures were taken of each wood chip sample. Then machine vision algorithms were derived from the colour information each picture contains. With these algorithms it was possible to determine different properties of wood chip samples. Finally the developed machine vision functions were verified and the suitability of machine vision identification was evaluated.

In order to create useful algorithms, each picture had to be analysed in the control PC where the distribution of colour tones is calculated. While doing this, unnecessary or even distracting information is filtered away, such as shadows. Parameters such as particle size can be calculated from the remaining picture.

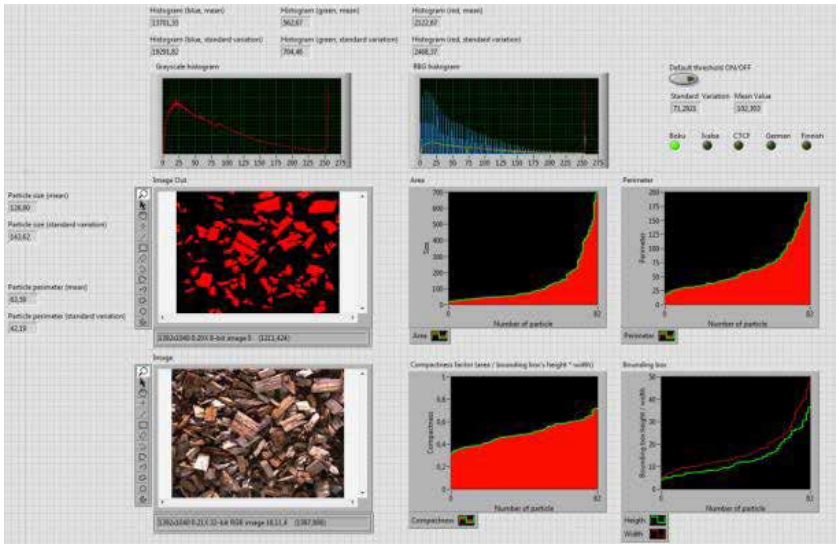

Figure 28. Machine vision results on a LabVIEW control screen.

The used identification function of wood chips is based on the mean value and standard deviation of colour tones. This means in practice that different colours are studied and identification of wood chips is done by using this information. Identification cannot be based on particle size because it varies significantly, depending on the chipper or grinder being used for comminution of wood.

Different colour tones are affected by several ambient factors like lighting, moisture content of chips, geometry and camera settings (lens opening, exposure time, etc.). When creating identification functions, these factors should be known and they should be kept as stable as possible. In our case, moisture of wood chips varied significantly between the samples. This was not a big problem, however, because moisture was one thing that we wanted to test, whether it is possible to determine moisture content with machine vision. Yet it should be noted that moisture affects the colour of wood chips, and therefore if the primary goal is to distinguish the type of wood chips, for example different wood species or stem wood from logging residues, moisture of each sample should be the same. On the other hand, if wood chips with different moisture contents are to be distinguished, the type of each wood chip sample should be known. In other words, because the identification of wood chips with machine vision is based on the type and colour tones of wood chips, either of the two variables has to be known in order to reliably determine the sample. Unfortunately, impurities and stains on wood chips easily increase the reliability of machine vision identification.

In our tests, the colour tones of different wood chips were often very similar, which made the identification of chips very challenging. The created algorithm might accidently find another ‘type’ or ‘species’ in the sample or mix two similar types. On the other hand, differences in shapes or ‘odd’ particles like needles help the identification if these variables are known.

Results of colour distribution of wood chip samples with similar moisture contents is shown in Table 18. The colour tone may vary between 0 to 255, where 255 is the lightest and 0 is the darkest tone.

Then limit values of the standard deviation and mean value of colour tones were set. They were set based on the results of the four photographs taken from each sample, according to the highest and lowest measured value. When these limit values were set, the machine vision system was able to identify the tested samples. However, if the colour tone values were similar with different samples, the system could not make a distinction between the samples. Therefore some identifications proved to be wrong, as seen in Table 19.

Table 18. Results of colour tone distribution of three types of wood chips.

Sample	Moisture content MC (%)	Mean value	Standard deviation
Boku1	30	102	71
Boku1	30	107	73
Boku1	30	101	67
Boku1	30	99	66
Mean Boku		102.25	69.25
CTFC1	30	75	59
CTFC1	30	74	58
CTFC1	30	69	55
CTFC1	30	70	56
Mean CTFC		72	57
FinRankahake1	31	91	67
FinRankahake1	31	97	70
FinRankahake1	31	97	69
FinRankahake1	31	93	69
Mean FinRankahake1		**94.5**	**68.75**

Figure 29. Photos of wood chip samples. Left CTFC1, right FinRankahake1 and middle photoBoku1

Table 19. Results of machine vision identification of different wood ship samples.

Sample	Standard deviation of colour tones	Mean value of colour tones	Machine vision system identification
Boku1 - MC 30	69	99	Boku/FinRankahake
Boku1 - MC 30	67	101	Boku
CTFC1 - MC 30	55	66	CTFC
CTFC1 - MC 30	55	70	CTFC
Ivalsa1 - MC 36	58	74	CTFC
Ivalsa1 - MC 36	59	77	CTFC/Ivalsa
FinRankahake - MC 31	68	96	Freiburg/FinRankahake
FinRankahake - MC 31	71	96	Boku/FinRankahake
Freiburg - MC< 15	63	86	-
Freiburg - MC < 15	61	87	-

10.3 Determining moisture of wood chips

Determining moisture of wood chips with machine vision rests on interpreting the distribution of colour tones of wood, like identifying different wood chips. Usually, wood chips are darker the higher their moisture content is. This is clearly seen Figure 30.

It was not possible to make any moisture content scale based on colour tones because a limited number of wood chip samples were analysed. In fact, in most cases samples represented just two moisture content levels. Only Finnish samples had more variety. However, in these tests the aim was to study whether it is possible to determine general differences in moisture with a machine vision system. Generally speaking, as stated before, the wetter wood chips are the darker they appear. Unfortunately, if there are impurities, large amounts of bark or staining by bark, colour tones are darker, thus indicating wetter chips. This naturally limits the accuracy of machine vision to determine moisture contents.

Some results of machine vision functions are summarized in Figure 31. As expected, they seem to strongly support that when chips are wetter the standard deviation and mean value of colour tones are smaller, thus making the picture darker. Therefore it can be concluded that moisture content can be measured with machine vision, at least on a rough scale.

FinRankahake, MC 31% FinRankahake, MC 41% FinRankahake, MC 49%

Figure 30. Finnish stem wood chips with differing moisture content.

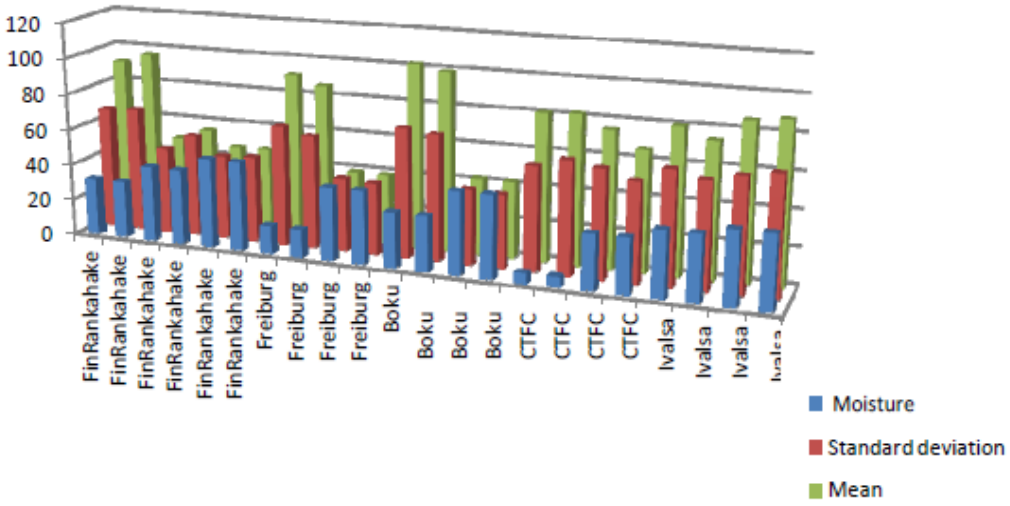

Figure 31. Standard deviations and mean values of the studied wood chips with different moisture contents measured by the test machine vision system.

10.4 Determining the particle size of wood chips

In order to measure or determine differences in particle sizes of wood chips, another algorithm was created, based on bigger and more outstanding wood pieces. To make the dominant pieces stand out shadows and very small wood pieces were removed from the picture. The modified picture rendered information on wood chips regarding surface area, circumference, length, width and compactness (i.e. area-circumference ratio).

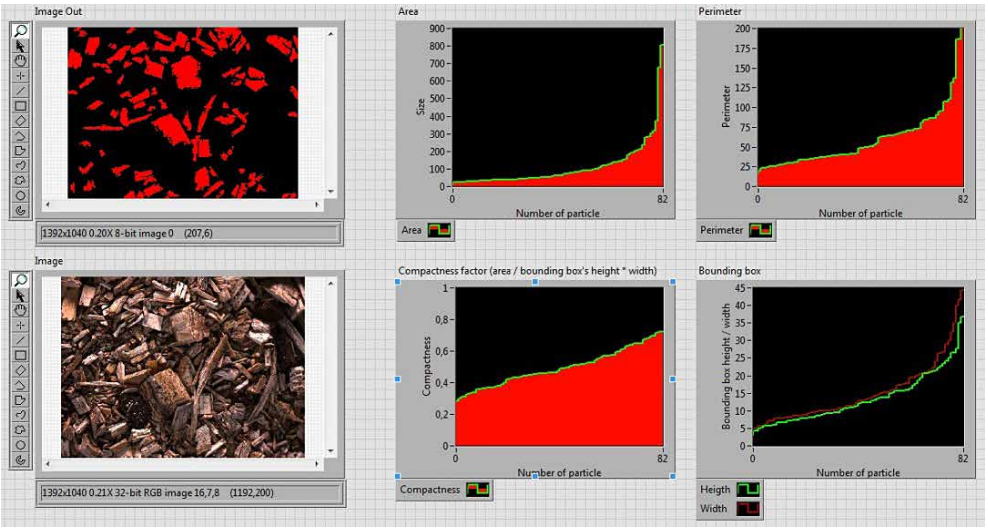

Figure 32. A sample picture of particle size determination taken from the control panel of the machine vision test system.

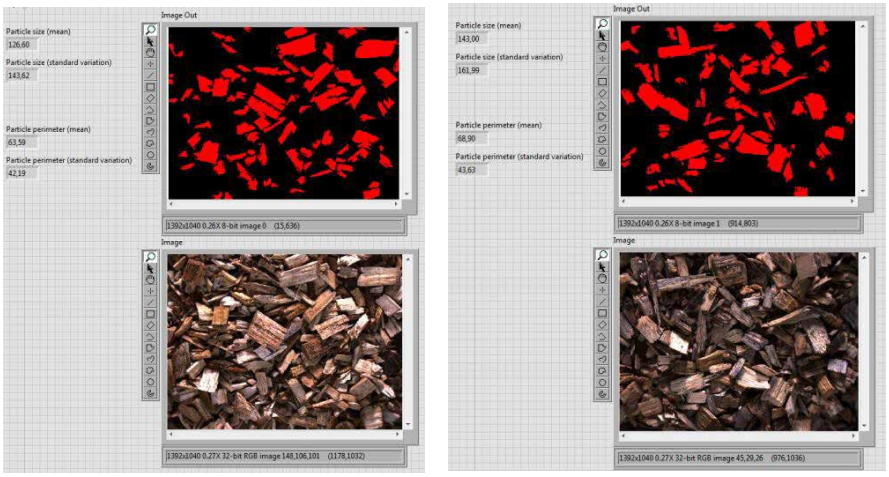

Figure 33. The original and processed (in red colour) particle size pictures.Results of particle size distribution are summarized in Table 20. It was challenging to 'measure' (determine) particle sizes because wood chips vary a lot in size and shape. Therefore the size values, presented in colour tone digits, are only estimates. Yet if compared to the pictures above, estimates seem to match quite well.

Table 20. Standard deviations of wood chip size distributions of analysed samples (value range 0–255 color tones). High standard deviation represents a large variety of wood chip sizes and shapes.

Sample	Standard deviation (surface area)	Standard deviation (circumference)
Boku1	144	42
Boku1	151	46
Boku1	122	34
Boku1	137	37
Mean value	138.5	39.75
CTFC1	162	44
CTFC1	160	42
CTFC1	143	43
CTFC1	134	42
Mean value	149.75	42.75
Ivalsa1	241	54
Ivalsa1	209	48
Ivalsa1	147	49
Ivalsa1	171	47
Mean value	192	49.5
Freiburg1	93	38
Freiburg1	95	35
Freiburg1	87	33
Freiburg1	98	34
Mean value	93.25	35
FinRankahake1	105	36
FinRankahake1	95	32
FinRankahake1	102	39
FinRankahake1	120	41
Mean value	105.5	37
FinHakkuutähdehake	240	78
FinHakkuutähdehake	287	87
Mean value	263.5	82.5

Again, moisture content and staining by bark in particular, affect the accuracy of machine vision in determining the size of wood pieces. Loose bark stains wood pieces, making them darker. Sometimes these darker pieces or parts are cut out as shadows in picture processing. Similarly if two or more pieces are lined up next to each other, they can be considered one big piece of wood. On the other hand, differences in wood chip types like stem wood chips or chips made from logging residues do not seem to affect picture processing very much, and therefore measuring results are quite similar with different wood chips.

11 Measuring the volume of a fuel wood load

In order to test a concrete and applicable machine vision system, several affordable contemporary cameras were considered. So called 'Time of Flight (TOF)' measuring technology was chosen because in addition to traditional grey scale picturing, TOF is able to give distance information about the object. In other words, it is possible to measure a grey scale value and distance value for every pixel of the object. With this information the volume of biomass in a vessel can be estimated for example.

Before setting up the test facilities at VTT, the camera and different picture geometries were tested at JAMK. All pictures were taken with a HALCON photography program and they were analysed with a National Instruments Vision Assistant program.

As mentioned, actual testing was done at VTT where it was possible to photograph bigger wood chip loads and to simulate authentic chip delivery situations. For this, the camera was installed on a passenger crane lift as high as five to six meters. This height was needed to be able to photograph the entire container at the same time. However, pictures were also taken from different sections of the chip load. The volume was also measured manually for comparison. The height calibration was done by taking pictures of the floor from measured heights. Furthermore, the system was also tested outdoors in bright daylight.

Measuring distances with a TOF camera is based on measuring the phase difference of sent and received light signals. The camera has an integrated infrared light source that sends light signals and a sensor that receives them. The resolution of the camera is 176 x 144. Each pixel gives distance information and therefore 25,344 distance values were acquired in total. These values have to be scaled to match values in reality. In practice, each picture is processed like any grey scale picture knowing that pixels contain distance information in relation to the camera. The scaling is seen in Figure 35 that presents pictures taken of the floor from certain distances.

Figure 34. The machine vision testing environment at VTT Jyväskylä. Source: Juho Riekkinen.

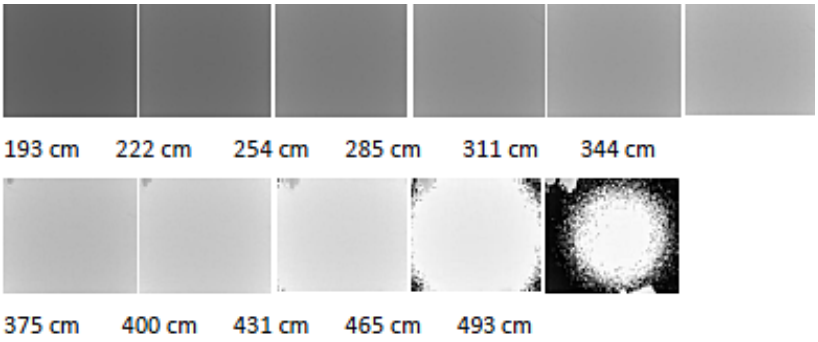

Figure 35. A sample of scaling pictures.

In order to scale grey scale pixel values ranging from 0 to 255, a coefficient had to be calculated. We get this coefficient by simply dividing the scaling distance by the mean value of the grey scale tone value distribution. With these coefficients it is very easy to scale any pixel value and get the real distance from the camera.

In the beginning pictures, were taken of the whole wood chip container. In order to do this, the camera had to be lifted to a height of 5.5 meters. However, this was out of the measuring range (0.3–5.0 m) according to the manufacturer of the camera. Therefore it was decided to take three pictures of each load. Then the longest distance from the bottom of the container was

4.6 meters and the shortest distance from the top of wood chips was about 3 meters. The photographing was repeated several times, to make sure the whole load was properly photographed.

Table 21. Coefficients to calculate the real distance from the camera.

Mean value of GS tone distribution	Distance (cm)	Distance / Mean value of GS tone distribution
173.98	344.00	1.98
190.96	375.00	1.96
203.35	400.00	1.97
219.83	431.00	1.96
237.02	465.00	1.96

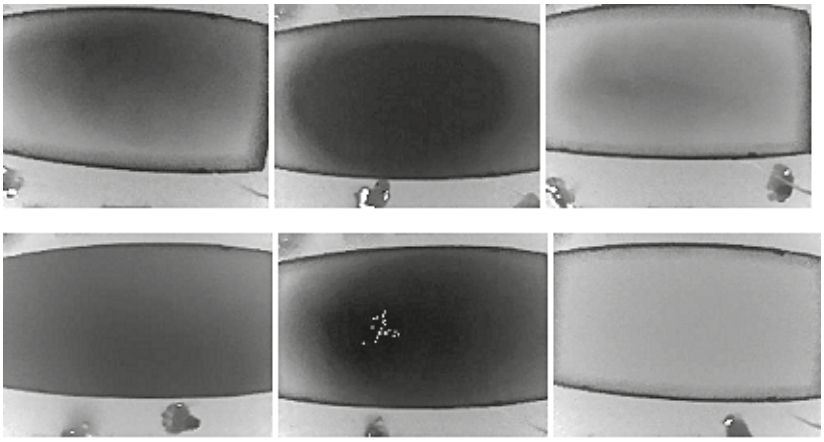

Figure 36. Pictures of wood chip loads (whole container). Dark = high or full load, Light = low or empty load.

Figure 36 illustrates TOF pictures of two wood chip containers. The darker the pixels are, the closer the object is to the camera. Both wood chip loads were determined manually by measuring the vertical distance from wood chips to the top of the container from 45 places (5 x 9). The mean values of the grey scale tone distribution from the corresponding places were chosen by the machine vision program for comparison. With the distance coefficients determined earlier it was possible to calculate the real distance from each measuring spot to the camera. By knowing the distance from the camera to the top of the container and the dimensions of the container (1.51 x 2.41 x 5 m), it was possible to determine the total volume of wood chips in the load (= mean values of load heights x width of container x length of container).

Distance values taken from machine vision pictures depend on what exact places they have been chosen from because each value is a sample representing an area of 0.45 x 0.56 meters in this case when 45 samples were taken. It is possible that the load 'height' fluctuates in this area and therefore this kind of manual measuring may not be very accurate. Also, taking pictures of exactly the same places as measured manually would have been very time consuming. However, for this study that aims to find out whether and/or how machine vision technology can be used to determine wood chip load volumes, this type of testing was considered adequate.

The measured volumes of container 1 varied between 8 to 10 m^3 depending on the size and location of the measuring areas. The volumes of container 2 varied from 11.5 to 13.5 m^3. In comparison, manually measured loads were 9 m^3 and 11 m^3 respectively, meaning that machine vision measurements corresponded well with manual ones.

In addition to testing the TOF camera indoors, some pictures were also take outdoors where the system was exposed to direct sunlight. Unfortunately, direct sunlight causes most pixels to appear completely light, thus making the distance determination impossible. In Figure 37 it can be seen how shadows render some distance information but other areas appear completely white with no grey scale tone values.

Furthermore, some pictures were taken of a moving chip truck but pictures turned out blurred and therefore distance determination became impossible.

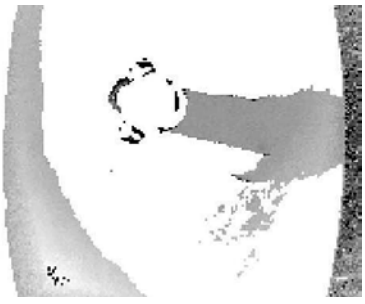

Figure 37: A picture taken in the sunlight with a TOF camera. A man is standing on the top of the wood chip load.

Figure 38: A TOF picture taken of a moving chip truck.

12 Wood chip analysis using near-infrared spectroscopy

The applicability of near-infrared (NIR) spectroscopy in the analysis of the moisture level of wood chips was briefly tested within the current INFRES project. The motivation for and challenges involved in using NIR in moisture analysis applications are given in the next two sections. Then, the NIR instrument utilized in the study is presented followed by presentation of the results from moisture analyses and classification tasks. Finally, the opportunities and challenges of NIR technology in wood chip analysis are listed as conclusions.

12.1 Moisture analysis using NIR

Near-infrared spectroscopy (NIR) is a field of vibrational spectroscopy which is widely used in the analysis of the chemical composition of various solid materials. Especially those chemical compounds which include N-H, O-H and C-H bonds in their molecular structure exhibit characteristic vibrational modes (overtones and combination modes) which are activated by electromagnetic radiation in the NIR wavelength range 800–2500 nm. The compounds may thus be identified and their relative concentrations may be quantified via observing the absorption of radiation by the sample in the NIR spectral range (Siesler et al. 2002). Due to the requirement for little or no sample preparation prior to measurement and its capability for analysing moving samples in a non-contact manner, NIR is often the method of choice in industrial inline process monitoring applications (Workman 1993). Examples include paper web moisture analysis during the paper manufacturing process (Paaso 2007) or heatset offset printing process (Tåg 2010), and real-time monitoring of the moisture level of pharmaceutical granules during a fluid-bed drying process (Nieuwmeyer et al. 2007). Indeed, due to the strong characteristic absorption bands of water at 1445 and 1950 nm (see left-hand plot in Figure 39), NIR is especially suitable for the analysis of the moisture content of solid samples.

NIR moisture measurement can be very accurate; in paper measurement applications, typical detection limits fall below 0.1% w/w of moisture (Tåg 2013). Ideally, due to the similar chemical composition between paper and wood chips (both contain mainly cellulose), similar moisture calibration methods are expected to be applicable, and similar accuracies are expected in the NIR analysis of moisture levels of both sample types (assuming that the chemical heterogeneity and the irregular surface shape of the wood chip samples do not distort the measurement). It must be noted that the information depth of NIR radiation in diffuse reflectance measurement of solid materials is generally between 100–1000 μm (see (Berntsson et al. 1999) for pharmaceutical materials), depending on the absorption and scattering properties of the sample at the given wavelength. Hence, NIR may only be used to characterize the very surface of the solid sample. The measurement may be assumed to be representative only if the chemical composition (e.g., moisture distribution) is homogeneous inside the sample.

NIR spectra of solid samples measured in diffuse reflectance mode are conventionally subjected to the logarithmic pseudoabsorbance transform equation prior to analysis. The pseudoabsorbance value at wavelength is obtained via the transform equation

$$A(\lambda)=[\text{“log”}]\_10\ (1/R(\lambda)\ )=[\text{“log”}]\_10\ ((W(\lambda)\text{-}D\_w\ (\lambda))/(I(\lambda)\text{-}D\_i\ (\lambda))) \quad (1)$$

where R(λ), W(λ) and I(λ) are reflectance, white reference and raw intensity values, respectively, at the wavelength λ. The reflectance expresses the ratio between the (dark-corrected) raw signals measured from the sample and from a white reflectance standard, and it (raw) gets dimensionless values above zero (usually below one). The raw measurements W(λ) and I(λ) (and their respective dark current measurements D_w (λ) and D_i (λ)) are expressed in the units of analogue-to-digital (A/D) counts and their levels are proportional to the light power incident on the detector at wavelength λ. The subtraction of the dark current level eliminates offset caused by the noise which is present in the signal given by the detector even when there is no light power shone on it. It should be noted that reflectance value R(λ) decreases whereas pseudoabsorbance value A(λ) increases when the intensity of back-scattered light decreases.

The motivation for using pseudoabsorbance units in the analysis of NIR spectra comes from the Beer-Lambert law (Siesler et al. 2002) of exponential light attenuation for clear (non-scattering) absorbing samples (such as clear liquids)

$$\text{“}Tc(\lambda)=\text{”}\ [(I(\lambda))/(I\_0\ (\lambda))=10]\text{^}(-\epsilon(\lambda)lc) \tag{2}$$

where the transmittance of the clear sample at the wavelength λ, Tc(λ) (the subscript c stands for clear sample), is expressed as the ratio between (the dark-corrected) sample signal I(λ) and the (dark-corrected) white reference I0(λ). When the multiplicative inverse of Tc(λ) is subjected to a 10-base logarithm, the obtained number – the absorbance value at the wavelength λ – is linearly proportional to each of the three factors in the exponent: ε(λ) is the molar absorptivity of the absorbing component at the wavelength λ, l is the optical path length and c is the molar concentration of the absorbing component. If the measured sample is a mixture of several absorbing species, the absorbance value of a clear sample at the wavelength λ may be written as the linear sum

$$A\_c\ (\lambda)=l\sum\_i\ [\varepsilon\_i\ (\lambda)\ c\_(i\ )] \tag{3}$$

which is linearly proportional to the concentrations of each of the light-absorbing components.

Easy and fast linear algebra is thus physically justified in extracting the concentrations of the individual chemical components from the absorbance spectra. When the logarithmic absorbance transform is applied to the reflectance or transmittance spectra of turbid (strongly scattering) liquids or solid materials, the units of the resulting spectra are said to be pseudoabsorbance. Although the Beer-Lambert law does not strictly apply to turbid samples, similar linearity (see Eq. (3)) is often assumed to prevail also in the pseudoabsorbance spectra – hence the motivation for using the transform.

When variations in moisture content can be expected to be the largest source of variation in the analysed samples, and when the chemical composition of the surrounding sample matrix may be assumed to remain relatively stable (chemically), the moisture content of the sample material is often characterized via inspecting the intensity (height or area) of the characteristic absorption band of water at 1950 nm (see rightmost plot in Figure 39). The pseudoabsorbance level gets relatively higher values (when compared to surrounding baseline points) when the sample absorbs more NIR radiation at the given wavelength. This is evident when the NIR spectra of two paper samples containing 0 and ~5% w/w of moisture are compared (see left and center

plots, respectively, in Figure 39): the characteristic 1950-nm absorption band of water is evident in the latter whereas it is absent in the former.

In the NIR analysis of paper moisture, it has been experimentally found that certain features extracted from the NIR spectra exhibit exceptional selectivity towards the true underlying moisture percentage of the sample. One such feature is the ratio between the baseline-corrected areas of the NIR absorption bands of water (at 1950 nm) and cellulose (2120 nm), as is visualized in the center plot of Figure 39. This moisture-selective ratio feature (henceforth named as WCR, water-cellulose-ratio) is given by "WCR"=A_w/A_c , where A_w (water band area) is the yellow area between the blue pseudoabsorbance spectrum and the cyan baseline level, and A_c (cellulose band area) is the green area between the blue spectrum and the cyan baseline level. The cyan baseline level (denoted by m_b) is calculated as the mean pseudoabsorbance value in the red region which contains no notable absorption bands. The subtraction of the baseline level and the division with the cellulose band area make the measurement of the intensity of the water absorption band more robust towards several disturbances which have an effect on the measured NIR spectrum. These sources of variation include light scattering effects (caused by, e.g., variations in porosity), instrument drift (e.g., variations in illumination power), and uneven illumination (e.g., dark shadows between particles). The right-most plot in Figure 39 displays a calibration fit between the WCR value and the reference (true) moisture level of the corresponding paper sample. It is seen that WCR correlates positively with the true moisture level and that a polynomial function may be used to very accurately describe this (non-linear but monotone) relationship. The measurements in Figure 39 have been conducted on paper samples, but similar phenomena are expected to be observed also in the case of wood chips. As a conclusion, NIR is a secondary measurement method which needs to be calibrated against a primary laboratory moisture analysis method, which, in the case of paper and wood chip samples, is often the well-known gravimetric (loss-on-drying) method.

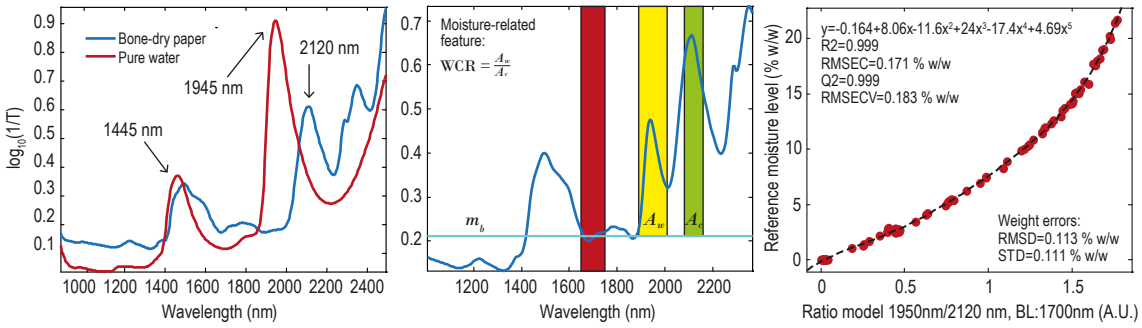

Figure 39. (Left) NIR absorbance spectra of pure liquid water (room-temperature) and printing paper (80 g/m^2), which has been dried into ~0% w/w moisture level, are displayed. In essence, the NIR spectrum of the dried paper exhibits the characteristic NIR absorption spectrum of cellulose. The 1950-nm absorption band of water exhibits good contrast against the cellulose baseline, since there is no overlap between the absorption bands of the two materials at this spectral location. (Center) A typical NIR absorption spectrum of paper (at ~5% w/w moisture level, room-temperature) is displayed. The calculation of the moisture-related feature (water/cellulose NIR absorption band ratio, WCR) is depicted (see main text for explanations). (Right) The reference moisture level of 61 paper samples is plotted against the corresponding water/cellulose band ratio values. A 5th order polynomial calibration function describes the relationship between the variables well. The data in this figure are taken from a previous project at VTT which focused on the analysis of paper moisture level using NIR.

12.2 Characterization of wood chips using NIR

The utilization of NIR spectroscopy in the characterization of wood chips at a biofuel power plant involves several challenges, which requires that the NIR measurement solution must be tailored to the given application. These challenges are listed next along with some references to literature where possible solutions to them are proposed. First, the analysed sample materials (wood chips) are often very heterogeneous: they may contain stem wood, bark, needles, small branches, etc., which all exhibit slightly different NIR absorption spectra. Moreover, a single biofuel plant must process wood chips made from several wood species which again have characteristic NIR spectra. In fact, it has been demonstrated that wood types and species may be very accurately identified based on their NIR spectra, irrespective of their moisture level (Tsuchikawa 2003). However, it has been also demonstrated that the inclusion of several wood species in the calibration training set facilitates the construction of a global NIR moisture calibration model which is insensitive to the wood type (Antti et al. 1996). The final option is to construct separate calibration models for each and every wood type, which is a laborious task. In any case, accounting for the differences between wood types must be accounted for when NIR moisture measurement solution is developed for wood chip applications. The final solution must be tailored according to the needs of the final application in the most economical way.

Second, it may be required that the NIR measurement be conducted outdoors. The ambient temperatures encountered in Scandinavia over the year range between -30 °C and +30 °C. It is well known that the characteristic NIR absorption spectrum of water changes drastically when the temperature is changed, especially when the changes occur around the freezing point between solid and liquid states of water. The utilization of a single NIR moisture calibration model becomes impossible even when the temperature variations are small (Thygesen et al. 2000a). Thus, temperature variations is another factor which must be taken into account in the NIR method development – either via ensuring that the samples be always stabilized into the same temperature before the NIR measurement, or via desensitizing the NIR moisture calibration model towards temperature changes (Thygesen et al. 2000b).

Third, the sample materials (wood chips) are very heterogeneous also physically. There are large variations in particle size and the measured sample surface is very uneven. Thus, the NIR sensor must be robust against baseline variations, i.e., changes in the probe-to-sample distance. Moreover, there may be dark shadowed regions between the wood chip particles which results in a low signal-to-noise ratio at these locations. Thus, it is mandatory that part of the collected spectra be automatically discarded when the intensity of backscattered light is too low.

Fourth, it is well-known that the NIR reflectance measurement gathers information only from the outermost layers of the solid sample. For example, the information depth for NIR radiation is only between 100–1000 μm in pharmaceutical powders (Berntsson et al. 1999). If the wood chip particles have an inhomogeneous radial moisture distribution, the NIR measurement is not representative. If inhomogeneity is suspected, it may be wise to let the samples stabilize in a closed plastic bag for several hours before the NIR measurement.

12.3 NIR instrumentation: chemical imaging and multipoint measurements

In this preliminary study, the applicability of NIR in the characterization of wood chips was conducted using an NIR chemical imaging (subsequently abbreviated as NIR-CI) system. The NIR-CI measurement produces a three-dimensional data structure, a spectral image, of the measured sample. The first two dimensions of the spectral image consist of the spatial dimensions of the image, and the third dimension is the spectral dimensions which contains several wavelength channels. In essence, one obtains a full NIR spectrum at each spatial pixel of the image. In addition to the chemically sensitive NIR spectroscopic analysis, one may hence study and visualize the spatial distribution of the target chemical components on the sample surface (a concentration map).

The utilized system is depicted in Figure 40. A commercial line-scanning (also known as push-broom imaging) spectral camera (SWIR, Specim Ltd., Oulu, Finland, see specifications in Table 22) was used in conjunction with a conveyor belt (Mini, ENP AB, Hjälteby, Sweden), and two rows of three 75-W halogen lamps (custom-made by Specim Ltd.). The conveyor belt was moving at the steady speed of 3 cm/s, and it provided the sample translation (scanning) required by the line-scanning imaging technology. The camera sees only a line of 320 spatial pixels at a time with a full 256-element NIR spectrum between 900–2500 nm recorded at each pixel. Hence, the sample needs to be scanned in front of the camera to get a full image of the sample. The halogen lamps were positioned 25 cm above the conveyor belt, and they illuminated the sample at the angle of 45°, whereas the camera looked directly downwards towards the sample (45°-0°-45° measurement geometry).

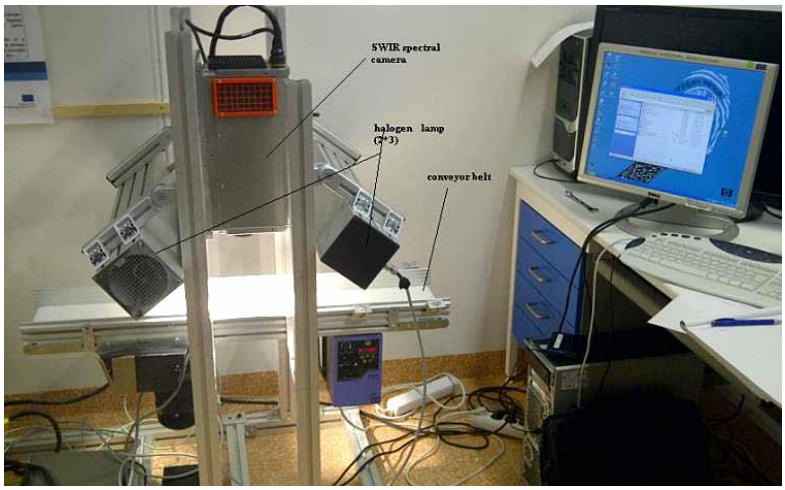

Figure 40. The near-infrared chemical imaging instrument at VTT Kuopio.

Table 22. Properties of the SWIR spectral camera.

Model	SWIR, Specim Ltd., Oulu, Finland
Spectral range	900-2500 nm (900-2200 nm with fiber-optics)
Detector	MCT (-70°C with 4-stage Peltier), 14-bit ADC
Pixels	320 (spatial) × 256 (spectral)
Maximum frame rate	100 frames per second
Model	SWIR, Specim Ltd., Oulu, Finland

The spectral camera was focused at 5 mm above the plane of the conveyor belt, the lens-to-sample distance was 18 cm, and the length of the imaged line seen by the camera was 96 mm (which corresponds to 320 pixels). The objective level resolution of the imaging measurement was thus 300 µm × 300 µm per pixel. The camera was used at the full data collection speed of 100 frames per second. As a result of the measurement, one obtains a 3-dimensional data structure of the size Y×320×256, where Y is the number of scanned frames which may be determined by the user. Each element of the 3D data cube contains a pseudoabsorbance value with the coordinates (y,x,w), where the two first coordinates correspond to a spatial location on the image (row and column), and the third coordinate is in the spectral dimension which is characterized by 256 equally-spaced spectral channels between 900–2500 nm.

The line-scanning spectral imaging system may be transformed into a multichannel spectrometer with the use of fiber-optics. The multipoint NIR instrument (also available at VTT Kuopio) is illustrated in Figure 41. The system is based on the same spectral camera (SWIR, Specim) as the NIR-CI system in Figure 40. Due to the addition of a fiber-optic front module (VTT), the detected light may be brought to the spectral camera from several measurement locations (possibly far apart from each other) via optical fibers. The measurement is conducted through fiber-optic probe heads which are connected to both illumination and collection fibers. The optics inside the probes project the illumination light onto the sample, and collect the back-scattered light from a small region (say, a diameter of 5 mm) on the sample surface into the collection fiber. The illumination may be arranged centrally with a multichannel light source (as is depicted in the image), or each probe may contain a separate halogen lamp (and a power source). Although this multichannel system is not used in this measurement campaign, it is mentioned here since the need for a multipoint measurement may arise in future wood chip analysis applications.

The line-scanning NIR-CI system is naturally suitable for conveyor belt applications where the wood chips are translated at a steady speed on a moving stage: the moving material may be scanned non-invasively at a distance of several tens of centimeters. Since NIR-CI also provides image information, it combines spectroscopy with machine vision, and thus makes the detection and identification of foreign materials and objects easier (when compared to single-/multi-point spectroscopy), and potentially facilitates the characterization of particle size and shape. The non-contact analysis of moving material streams is also possible with the MP-NIR instrument. Using fiber-optics, measurements may be conducted simultaneously at several locations, possibly at

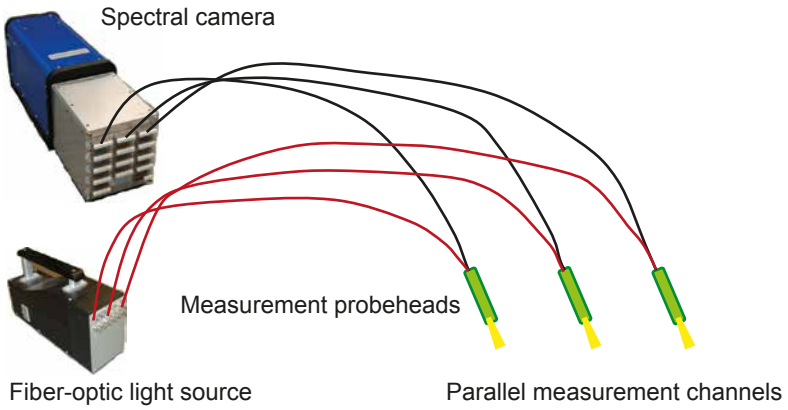

Figure 41 The multipoint near-infrared instrument.

different stages of the process (e.g., before and after a drying stage), making the collection of data cost-effective. It may be said that the MP-NIR instrument contains several single-point spectrometers in a single device. Moreover, the MP-NIR may be connected to an immersion probe, i.e., a rod which has a fiber-optic NIR sensor(s) at its tip or along its length. When this rod is immersed into a pile of wood chips, a moisture reading from the interior of the load may be measured, which facilitates the analysis of stationary wood chip loads. One must bear in mind that the NIR measurement (be it NIR-CI or MP-NIR) is always restricted only to the surface of a single wood chip (due to the limited information depth of NIR radiation in diffuse reflectance measurement).

12.4 Artificial demonstration: detection of moisture differences in spray-wetted sample

The capability of NIR to detect and quantify moisture in wood chips is first demonstrated with an artificial test. Wood chips (CTFC2, 5% moisture, Spain) were spread evenly onto the conveyor belt of the NIR-CI system, and the left half of the sample was spray-wetted. A photograph of the sample is visualized in the left-hand side of Figure 42. The wet region is seen to have a slightly darker colour shade when compared to the dry region. The detection of the moisture differences is thus possible with conventional machine vision systems operating in the visible wavelengths. This is due to the fact that the water replaces the air in the pores of the wood and thus reduces the difference between the refractive indices of wood fibers and the inter-fiber spaces (pores). This again reduces the light-scattering power of the sample (via reduced refraction) making it look darker (since less light is back-scattered from it). The moisture measurement based on the intensity of back-scattered light at visible wavelengths is thus indirect as it is based on detecting variations in the light scattering properties of the sample (which are, hopefully, caused by variations in moisture level). However, this indirect measurement is not selective since the light scattering properties and the colour shade of the sample may be affected by several other factors, as well, such as variations in sample porosity. NIR provides an advantage over visible-range imaging due to its chemical sensitivity: the NIR absorption of water may be measured directly and selectively.

To demonstrate the detection of moisture with NIR, the half-wet sample was also measured with the NIR-CI system. The resulting spectral data cube is visualized as a pseudo-RGB image (center image in Figure 42), where reflectance values at three wavelengths (here 1106, 1945 and 2315 nm, respectively) are used as red, green and blue coordinates. The wet region is easily distinguishable from the dry region via having a relatively higher red component. The pseudo-RGB images are only used as a tool for visualizing the NIR spectral data cubes, and no further analysis is conducted on them here. However, quantitative analysis of moisture level becomes possible when the moisture-selective spectral feature WCR is visualized as a map (see rightmost image in Figure 42). Since the WCR value is assumed to correlate positively and selectively with the true moisture level, the intensity image is thus a moisture map as it displays the spatial distribution (and the amount) of moisture on the surface of the wood chips. It is evident that NIR-CI is more powerful than visible-wavelength imaging in the detection and quantification of moisture in wood chips: the contrast between the wet and dry regions is higher in the NIR images.

A typical NIR spectrum of wood chips is illustrated in the left-hand plot of Figure 43. When compared with Figure 39, it is seen that the NIR spectra of wood chips and paper samples are very similar, mainly due to the presence of cellulose and moisture in both materials. It is thus expected that the utilization of the WCR as a moisture-selective feature is permitted in the analysis of wood chips, as well. Spectra picked randomly from the spectral image of the half- wet sample

(see Figure 42) are coloured according to WCR value in the right-most plot of Figure 42. It is seen that both water absorption bands (1445 and 1950 nm) increase in intensity as the moisture level is increased. The moisture level correlates with the spectral baseline level, as well: the pseudoabsorbance values in the region 1600–1800 nm (which does not contain strong absorption bands) generally increases with moisture level. This is due to the fact that the presence of moisture decreases the light-scattering power (as was discussed earlier in the case of visible-wavelength-imaging): lower intensity of back-scattered light means a higher average pseudoabsorbance level (higher spectral baseline level).

Figure 42. Demonstration of moisture detection with NIR. (Left) A photograph of wood chips on a conveyor belt is displayed. The left half of the particles has been spray-wetted which is seen as a slightly darker colour shade. (Center) The same sample was measured with NIR-CI and the spectral image is displayed here as a pseudo-RGB image using three reflectance values (at 1106, 1945 and 2315 nm) as RGB coordinates. The wet area has relatively higher red component. (Right) The ratio of water/cellulose NIR absorption bands is displayed as intensity image (moisture map). Red/blue colour means high/low moisture level at the corresponding location.

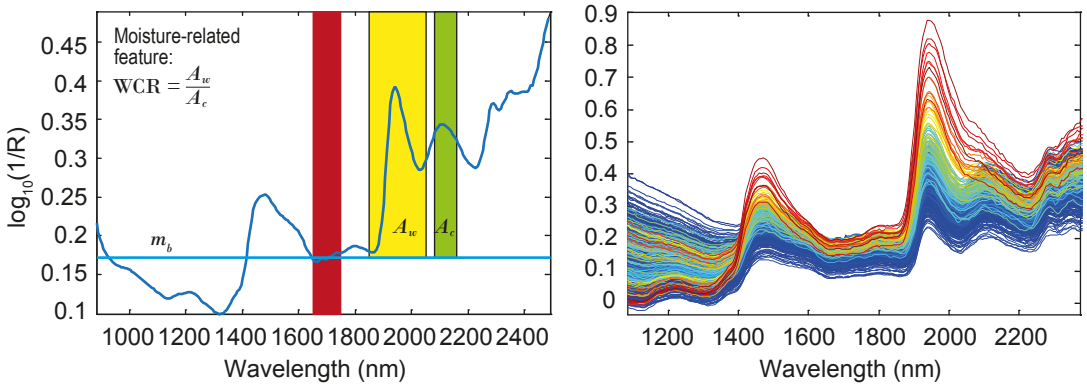

Figure 43. (Left) Typical spectrum of a wood chip is displayed. It is seen that the spectral shape is similar as that of paper sample (cf. Figure 39). Hence, the same moisture-selective feature WCR (ratio of water/cellulose NIR absorption bands) may be used in the quantification of moisture level in wood chips. (Right) Spectra picked from the NIR spectral image of the half-wet sample (cf. Figure 37) are displayed here. The spectra have been coloured according to the moisture- selective feature WCR.

12.4.1 The main measurement campaign

The current measurement campaign consisted of the NIR-CI measurements of typical wood chip samples which exhibited variations in the wood type as well as in moisture level. Eleven bags were received for NIR-CI analysis, each containing wood chips at a certain moisture level (1–2 moisture levels per sample type). These samples were the same samples as used for RGB measurements in Jyväskylä, excluding FinRankahake3 (cf. Table 23). The wood chips had been stored in closed plastic bags for several months prior to the NIR-CI measurements. Thus, the reference moisture level is only approximate: the moisture distribution inside the sample mass is likely to be very heterogeneous, and there is a chance that some of the moisture has evaporated despite the surrounding plastic bag. The presence of mildew or fungus was not visible to the human eye. However, some samples had regions which exhibited relatively high absorption in the 900–1100 nm spectral range. These regions may be mildew, and they are seen as blueish spots in the pseudo-RGB visualizations of the spectral images (see, e.g., the left-hand image in Figure 44).

The contents of each plastic bag were mixed by tossing and turning the bag prior to measurement. Three independent samples (~200 g each) were extracted manually from the center of the bag and they were measured in duplicate immediately after extraction. The second NIR-CI measurement was conducted immediately after the first one (without touching or re-arranging the wood chips), and its purpose was to study whether the moisture level of the sample changes as a result of the NIR-CI measurement. Only the first measurement of each sample is used in the subsequent analysis, unless otherwise specified. Typical NIR spectral image (visualized as a pseudo-RGB image), moisture map (as calculated in a semi-quantitative manner using the WCR) and the moisture distribution (histogram) are shown for the CTFC2 (Spain, 5% moisture) and logging residue (Finland, 49% moisture) samples in Figure 44 and Figure 45, respectively. To improve the accuracy of the moisture measurement, the image areas having a low signal-to-noise ratio (dark shadows) and those where the plastic conveyor belt was visible were eliminated from the data prior to analysis.

Table 23. Wood chips measured with NIR. The left column gives the name, brief description, and origin of the samples, whereas the right column gives the approximate reference moisture level.

Sample	Moisture (%)
Boku1 (stem wood chips), Austria	30
Boku2 (stem wood chips), Austria	45
CTFC1 (stem wood chips), Spain	30
CTFC2 (stem wood chips), Spain	5
Ivalsa1 (stem wood chips), Italy	36
Ivalsa2 (stem wood chips), Italy	40
Freiburg1 (stem wood chips), Germany	<15
Freiburg2 (stem wood chips), Germany	>30
FinRankahake1 (stem wood chips), Finland	31
FinRankahake2 (stem wood chips), Finland	41
FinHakkuutähdehake (logging residues), Finland	49

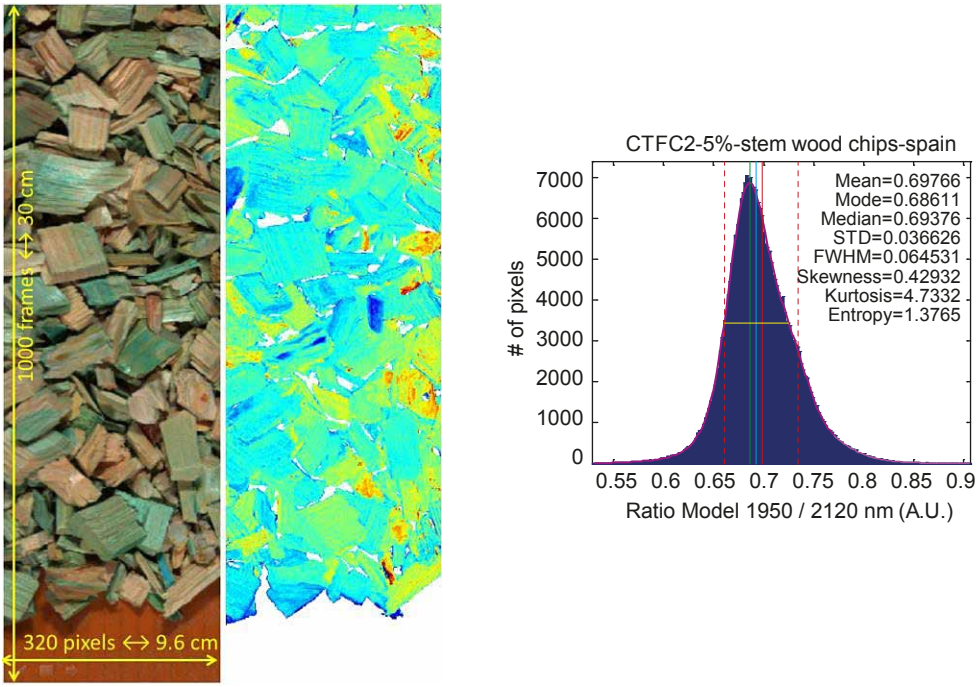

Figure 44. Visualization of the NIR-CI spectral image of a single sample taken from the CTFC2 bag (5% nominal moisture level). (Left) The NIR spectral image is visualized as pseudo-RGB image where reflectance values at 1106, 1737 and 2315 nm were used as R, G and B coordinates, respectively. The dimensions of the imaged are given in pixels and centimeters. (Center) The moisture map (as calculated with the water/cellulose band ratio) is visualized. The plastic conveyor belt and dark areas (shadows) have been removed prior to analysis. (Right) The histogram distribution of water/cellulose band ratio values from the moisture map is displayed along with some statistics. NB: these data correspond to a single measurement on a single sample. In total, three samples from each bag were measured in duplicate. The abbreviation (A.U.) stands for arbitrary units.

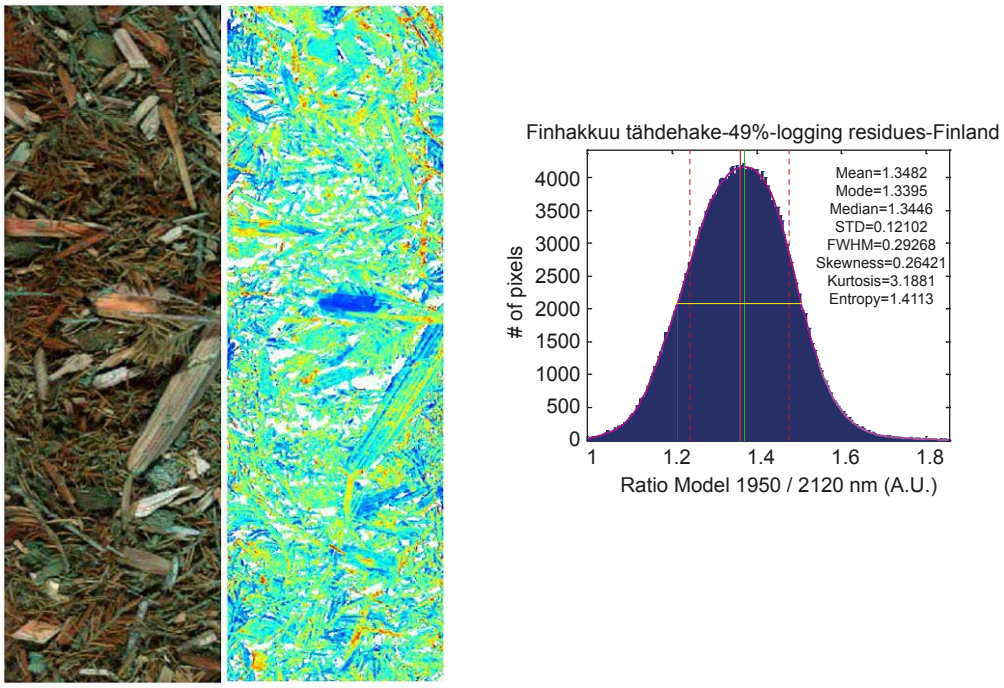

Figure 45. Visualization of the NIR-CI spectral image of a single sample taken from the bag containing logging residues (49% nominal moisture level). See the caption of Figure 43 for explanations. Note that the composition of logging residues is very different from the typical wood chips: there are more needles and small branches.

In the current study, only semi-quantitative moisture analyses were carried out. In other words, the WCR values extracted from the NIR spectra were analysed as such and they were not converted into absolute moisture percentages. The reason for this was twofold. First, there were no resources available for carrying out reference moisture measurements (with the loss-on-drying method). Accurate reference moisture values are needed in order to construct a calibration function (which was done for paper samples in the rightmost plot in Figure 39). It was also believed that the reference moisture values given for each bag were not accurate enough to permit the construction of a reliable moisture calibration model. Second, the sample set comprised six different types of wood chip samples each having different chemical and physical characteristics. Each of the bags contained different wood species as well as different mixture ratios of stem-wood, bark, needles and thin branches. It was observed that even though the WCR feature eliminates many small differences in the NIR spectra (viz. baseline offset and scaling differences), it will not be immune towards the large differences observed, e.g. between the NIR spectra of stem-wood and bark particles. In paper moisture analysis, separate moisture calibration models need to be constructed for each paper type (having differences in grammage and filler content). Similarly, it is believed that separate moisture calibration models need to be constructed for different wood species and wood types, as well. Optimization of the calibration procedure requires additional research effort, and it was out of the scope of this study.

Due to the semi-quantitative nature of the study, only relative differences in the moisture levels of the wood chip samples of the same type could be assessed. In Figure 46, the moisture distributions calculated over the three replicate samples are visualized for the two moisture levels of three wood chip types: Boku, CTFC and Ivalsa. As is expected, the moisture distributions of the samples with lower reference moisture values have smaller a mean value (they are more on the left). In the lower right-hand plot of Figure 46, the mean values and standard deviations of the distributions of the moisture distributions (calculated in a semi- quantitative manner with the WCR) of all eleven wood chip bags are visualized as coloured dots and error bars, respectively.

There is a clear correlation between the WCR value and the reference moisture level. The deviations from a perfect linear relationship are most probably caused by the different chemical and physical characteristics of different wood chip types (which affect the band ratio value) as well as errors in the reference moisture levels. It is very likely that same calibration fit may not be used for all wood chip types. It should be noted also that the standard deviations of the moisture distributions correlate positively with the reference moisture level. This is also natural, since the standard deviation should go to zero as the true moisture level of the chips approaches 0%, and it further reinforces our assumption that the WCR level correlates selectively with the true moisture level.

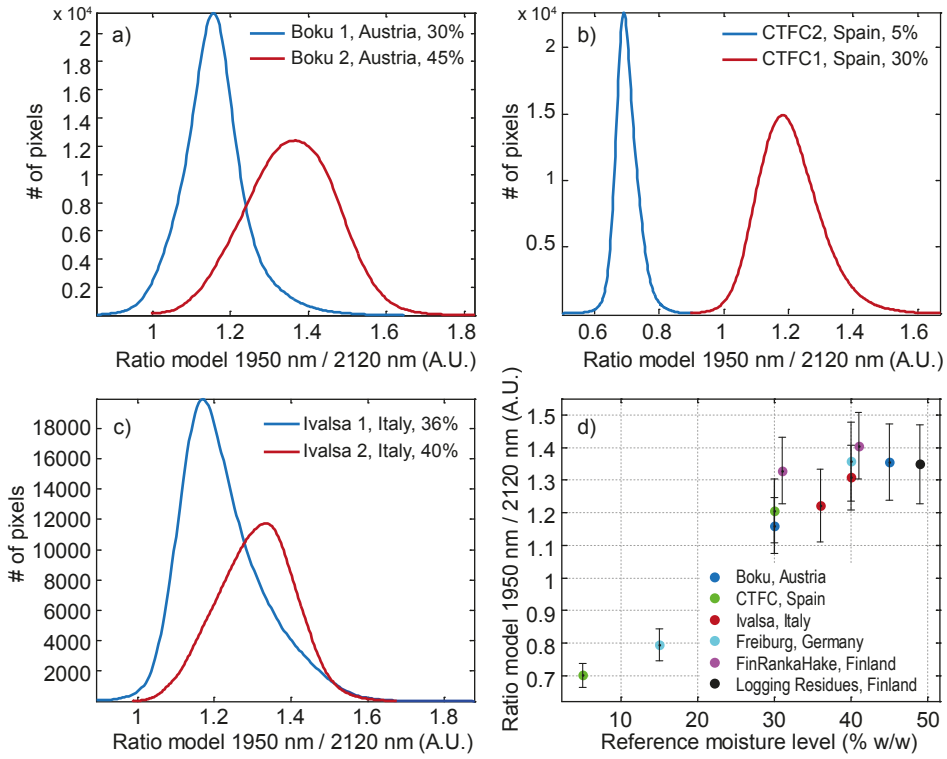

Figure 46. The moisture distributions (as quantified in a semi-quantitative manner with the water/cellulose band ratio) are displayed in histogram form for the following wood chip types (a) Boku, Austria; (b) CTFC, Spain; and (c) Ivalsa, Italy. Each histogram contains WCR values from three independent samples taken from each bag. The moisture-selective spectral feature (water/cellulose ratio) always behaved as expected in the case of all wood chip types: the samples with lower nominal moisture level always yielded lower water/cellulose ratio values. The mean values and standard deviations of the distributions are visualized as coloured dots and error bars, respectively, in (d). There is a clear correlation between the band ratio and the reference moisture level. The deviations from a perfect linear correlation are most probably caused by both the different chemical and physical characteristics of different wood chip types (which affect the band ratio value) as well as the errors in the reference moisture levels.

12.4.2 Invasiveness of the NIR-CI measurement: evaporation of moisture due to high-power illumination

To ensure that the power of light back-scattered from the analysed sample is sufficiently high, high-power halogen lamps must to be used in the NIR-CI measurement. In the current measurement set-up, the sample is illuminated with six 75-W halogen lamps from the distance of ~40 cm. Even though the measurement lasts only for 10–20 seconds per sample, the temperature of the samples increases notably during the measurement. This results in the evaporation of moisture. Of course, the evaporation occurs mostly on the surface of the wood chips, and the total mass of the sample material most likely decreases only slightly (the change in mass was not studied). However, since the NIR measurement sees only the very surface of the sample, the effect of evaporation (if it occurs) should be visible in the WCR parameter extracted from the NIR spectra. All thirty-three samples (eleven bags, three samples each) of the main measurement campaign were measured in duplicate to permit the analysis of the effect of evaporation caused by the high-power illumination. The second measurement was conducted immediately after the first one without touching the sample in between.

Typical results are visualized in Figure 47, where the moisture distributions of the duplicate measurements conducted on Boku1 (Austria, 30%) and FinRankaHake2 (Finland, 41%) samples are visualized. It is seen that the moisture distribution of the second measurement is always located slightly more to the left of the distribution of the first measurement: the distributions are highly overlapping but the mode of the distribution has clearly shifted towards the left. The NIR-CI measurements thus confirm the hypothesis concerning the evaporation of moisture caused by high-power illumination.

In Figure 48, the mean values of the moisture distributions of the first and second measurements conducted on the thirty-three samples of the main measurement campaign are plotted against each other. It is seen that the mean value of the first measurement is always slightly higher than that of the second measurement. The difference between the two mean values seems not to depend on the moisture level of the wood chips: the points in the plot are always located by the same amount below the diagonal line regardless of the moisture level (or WCR value).

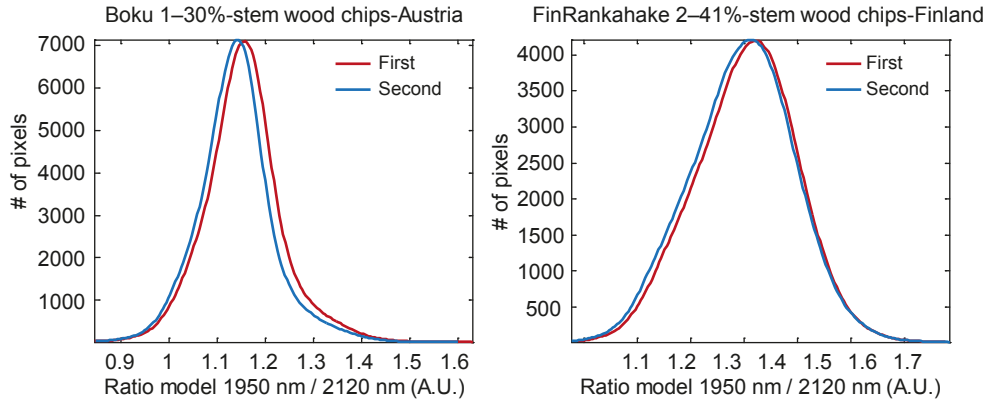

Figure 47. Moisture distributions (as calculated in semi-quantitative manner with the water- cellulose ratio feature) of two measurements conducted on the same sample for the samples from (Left) Boku1, Austria (nominal moisture level 30%), and (Right) FinRankaHake2, Finland (nominal moisture level 41%). The first and second measurements conducted on the same sample are plotted in red and blue colours, respectively. The second measurement was conducted immediately after the first measurement without touching or moving the wood chips in between. It is seen that the moisture distribution has been slightly translated towards left in the second measurement. The high-intensity illumination utilized in NIR-CI measurement thus evaporates a little bit of the moisture.

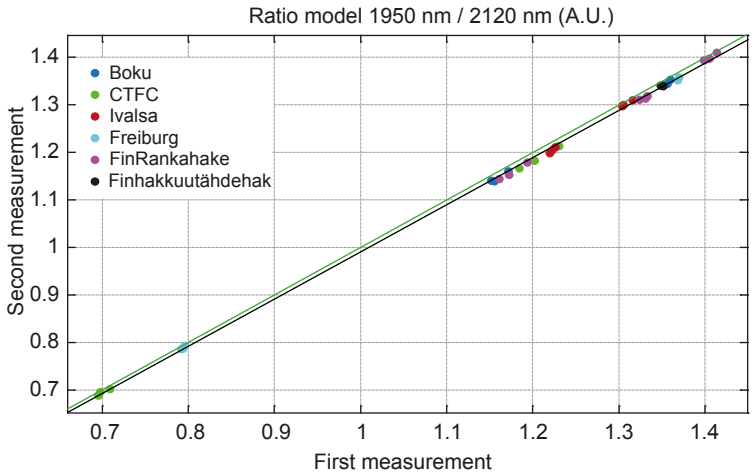

Figure 48. Mean moisture values (as calculated in a semi-quantitative manner with the water/cellulose ratio, WCR) of the two measurements conducted on each sample are plotted against each other. The value from first measurement is on the horizontal axis. The green line is the diagonal; ideally, all points should land on the green line. However, since the NIR-CI measurement slightly evaporates moisture from the wood chips, the mean moisture value from the second measurement is always slightly lower when compared to first measurement. The black dotted line is a linear fit between the two values.

As was mentioned above, the halogen illumination also most likely increases the temperature of the sample. The wood chip temperatures were not studied before and after the measurements, but fortunately, some information on the sample temperature may be extracted also from the NIR spectra. Since the vibrational states of molecules are strongly dependent on temperature, some NIR experts say somewhat sarcastically that every NIR spectrometer is also a thermometer (see (Lin et al. 1993) for demonstration). It is widely known that the two major absorption bands of water (located at 1445 and 1950 nm at room temperature) move towards smaller wavelengths (higher frequencies) as the temperature rises (Thygesen et al. 2000a). To figure out whether the temperature of the sample increases as a result of high-power halogen lamp illumination, the mean NIR spectra calculated over the two replicate measurements of each sample were compared to each other. A typical result is visualized in Figure 49, where the spectra from the two measurements on one sample of logging residues are visualized. When inspected visually, the two spectra overlap perfectly (left- hand plot). When the element-wise difference spectrum (first minus second spectrum) is calculated, it is seen that the second spectrum exhibits relatively higher pseudoabsorbance levels at 1415 and 1888 nm, since the difference spectrum is negative at these locations. These two locations are slightly to the left of the two major absorption bands of water. Thus, the absorption bands of water have moved towards smaller wavelengths as a result of heating. The NIR-CI measurement has thus a small effect on the sample temperature, although it is likely that the effect is so small that it does not affect the moisture measurement. If the NIR measurement is conducted outdoors, the expected sample temperatures encountered over the year range from -30 °C to +30 °C, which poses a disturbance several orders of magnitude larger than what is observed in laboratory conditions. However, desensitizing the NIR moisture measurement against large temperature variations is out of the scope of this project (see (Thygesen et al. 2000b) for proposed solutions).

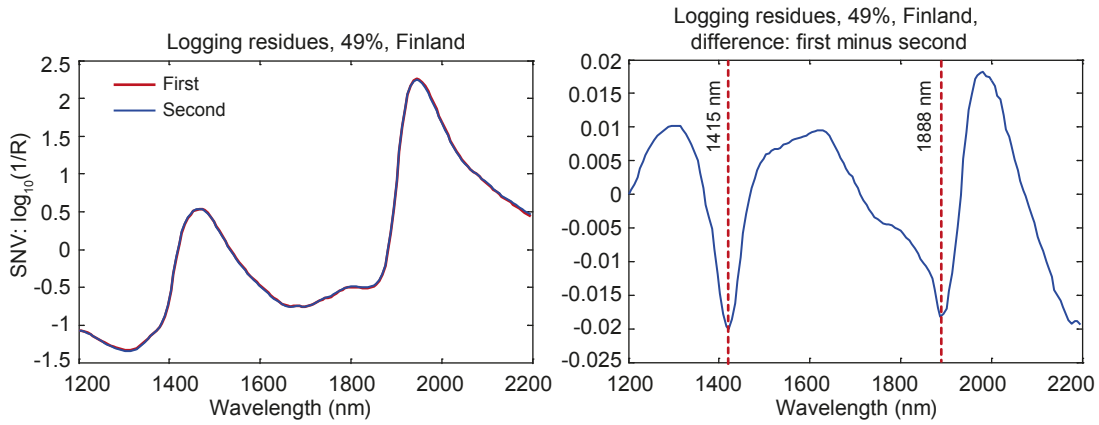

Figure 49. (Left) Mean NIR spectra calculated over the first and second NIR-CI measurements of logging residues sample (nominal moisture 49%). The second measurement was carried out immediately after the first without touching the wood chips in between. When inspected visually, the two spectra are perfectly overlapping. (Right) Element-wise difference spectrum: first minus second spectrum. It is seen that the second spectrum exhibits higher pseudoabsorbance levels at 1415 and 1888 nm, since the difference spectrum is negative at these locations. These two locations are slightly to the left of the two major absorption bands of water (1445 and 1950 nm at room temperature). Thus, the absorption bands of water have moved towards smaller wavelengths as a result of heating. The abbreviation SNV stands for standard normal variate transform in which the mean pseudoabsorbance level of each spectrum is translated to zero after which the standard deviation of the values is normalized to unity. This makes the visual comparison of the spectra easier.

12.5 Classification capabilities of NIR chemical imaging

The wood chip samples often are very heterogeneous. Even if the chips were produced from the same tree species, the samples contain particles that are vastly different in terms of visible colour, chemical composition, density, etc. Each bag of wood chips analysed during this project contained at least two of the following wood parts: stem wood, bark, needles and small branches. This heterogeneity poses a challenge for NIR analysis: the chemical and physical differences of different particles might require that different moisture calibration models be used for each particle type. Even though the WCR feature is selective towards the moisture level, it will most likely not be able to eliminate the differences in the NIR spectra imposed by different wood types. For example, the chemical and physical differences between stem-wood and bark particles may be visible in their respective NIR spectra. If the NIR-CI system is used in inline analysis of wood chip loads brought to a biofuel power plant, the system must be able to identify the identities of various particles presented to it and choose the corresponding calibration models to be used with each of them. Establishing a library of calibration models for different materials takes lots of work, and it is out of the scope of this project. However, it is demonstrated below that there is a need for separate calibration model between stem-wood and bark, and that the identification of different wood materials is indeed possible using NIR-CI measurement and subsequent data analysis.

In Figure 50, it is demonstrated that a separate moisture calibration model is needed for stem-wood and bark particles if the WCR value is used as independent univariate variable in a polynomial regression for predicting the true moisture level (the dependent variable). The sample (which was imaged with the NIR-CI system) contains both stem-wood and bark particles which are clearly separated into two regions. The bark particles get higher WCR values even though all particles in the image should have the same moisture level (since they have been in the same sealed plastic bag for several months). It must be noted, however, that in the fields of chemometrics and spectroscopic data analysis, there are methods available which are designed to eliminate the differences in the NIR spectra of two classes and to make the calibration model insensitive to these differences. For example, in (Antti et al. 1996), a single global calibration model was constructed via including several wood species in the calibration training set. In any case, it is clear that the heterogeneity of the wood chip samples must be taken into account somehow.

The left-most image in Figure 51 is a regular photograph taken of the stem-wood chips and bark particles picked from the bag containing CTFC2 wood chips (Spain, 5% MC). The stem- wood and bark particles are located in the upper and lower halves, respectively, of the image. The particles were measured with NIR-CI in this configuration after which a classification model (partial least squares discriminant analysis, PLS-DA, with four latent variables) was constructed between the spectra manually picked from upper and lower halves of the spectral image. The center image of Figure 51 shows the continuous output of the PLS-DA model (when applied to the training set). It is seen that the stem-wood and bark particles are well separable from each other based on this image.

The rightmost image of Figure 51 displays classification result obtained via thresholding the values in the center figure into two classes. The constructed classification model was also applied to a test set containing different stem wood and bark particles, and the classification was noted visually to be as good as in the training set (results not shown). There are some misclassified pixels in the center of the particles, however. The classification performance may be further improved (made more robust) via the utilization of image processing techniques. For example, all pixels within one segmented particle should be forced to have the same class. As a conclusion,

it may be stated that NIR spectroscopy may be utilized in automated detection of the wood chip type, which is a necessary prerequisite if separate NIR moisture calibration models must be used for different wood chip types.

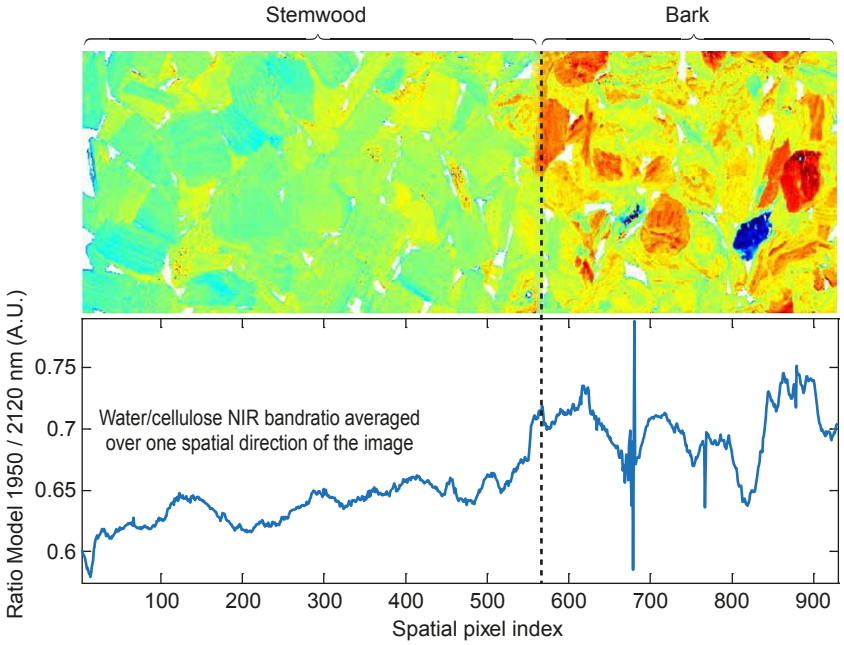

Figure 50. (Top) Intensity image visualizing the water/cellulose ratio (WCR) of the NIR spectrum at each pixel for the spectral image of stem-wood and bark particles. (Bottom) The WCR profile obtained via averaging the values over one spatial direction. The border between stem-wood and bark particles are denoted with dashed black vertical line. The WCR value of the bark particles is higher, even though the samples should be at the same moisture level.

Figure 51. Classification between stem wood and bark particles with NIR-CI. (Left) Photograph was taken of stem-wood chips and bark particles placed on the conveyor belt in separate groups. (Center) Continuous output of a linear classification model (PLS-DA) which was trained on this image. (Right) The pixels are classified into two groups via thresholding the values of the center image.

Another classification task encountered in the inline analysis of wood chips is the detection of foreign materials amidst the wood chips. The most common foreign particles are rocks which should ideally be identified and removed before the wood chip load is inserted into the boiler. This situation was simulated via placing eight small rocks (2–4 cm in diameter) next to the wood chips on the conveyor belt. In Figure 52, the obtained spectral data cube is first visualized as a pseudo-RGB image (left), where the eight rocks are easily seen. The detection of the rocks was conducted with principal component analysis (PCA). A PCA model (scores and loadings) was first created using a separate spectral image containing only wood chips (image not shown). The NIR spectra of the spectral image containing eight rocks amidst wood whips were then projected onto the affine space spanned by the three most significant principal components obtained from the first image. The squared reconstruction error (the Q statistic) was then calculated for each NIR spectrum in the test image, and its logarithm is visualized as intensity image in the center of Figure 52. The eight rocks are clearly seen as outliers, since the reconstruction error is larger for the spectra measured from the rocks. The rightmost image in Figure 52 is obtained via thresholding the values in the center image. The identification of the rocks via the outlier detection method (such as PCA's Q statistic) is thus possible. Note that the darkest pixels which correspond to shadows and some surface pixels of the dark-coloured rocks have already been removed prior to analysis due to their low signal-to-noise ratio. Again, the robustness of the rock-detection algorithm may be improved via the utilization of image processing routines. First, the borders of the particles (wood chips and rocks) should be identified. Then, the classification result (inlier or outlier) of all pixels inside each particle should be forced to have the same value.

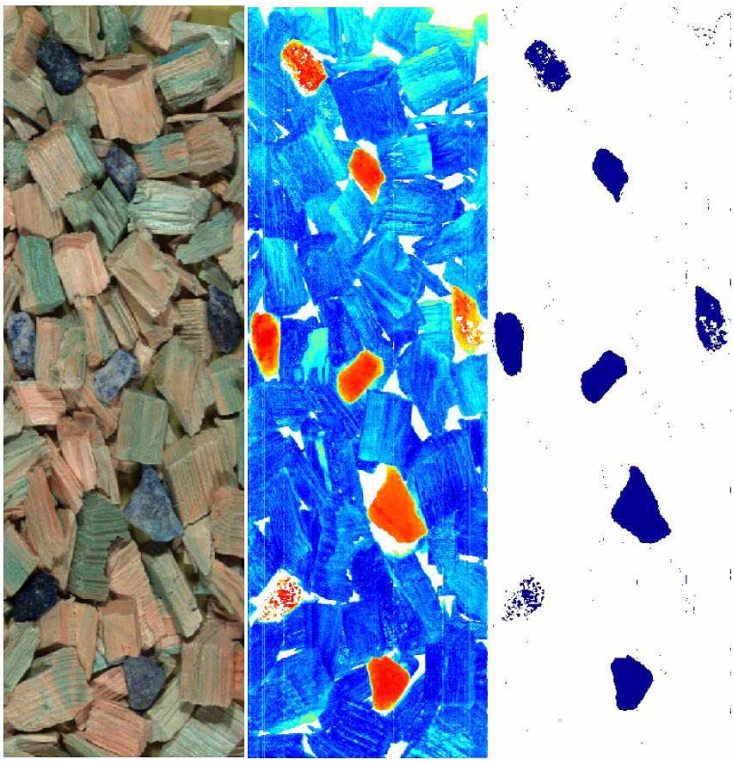

Figure 52. Detection of rocks amidst wood chips. (Left) Eight small rocks were placed on the conveyor belt containing wood chips (pseudo-RGB visualization of the NIR spectral image). (Center) Squared reconstruction error (Q statistic from PCA) of the spectra visualized as intensity image after logarithm transform. The rocks are clear outliers. NB: Some pixels have already been removed prior to analysis (elimination of dark shadows, dark rocks and plastic conveyor belt). (Right) Outlier pixels obtained via thresholding the values in the center image.

13 NIR spectroscopy conclusions

During the tests carried out in this study, near-infrared chemical imaging (NIR-CI) was demonstrated to be applicable for the analysis of the moisture level of wood chips. Several opportunities and challenges for the application of NIR technology in wood chip analysis were identified, and these points are listed in Table 24. As a major opportunity, the applicability of NIR spectroscopy in the non-contact analysis of moving materials has been demonstrated in earlier industrial applications. NIR is specifically sensitive towards moisture due to the strong characteristic absorption of water in the NIR spectral range.

The moisture levels predicted (in a semi-quantitative manner) from the NIR spectra measured on a wide variety of wood chips behaved expectedly during the main measurement campaign of this study: the water-cellulose band ratio (WCR) values were repeatedly ordered according to the reference moisture level within one wood chip type. Due to the chemical sensitivity of NIR spectroscopy, the classification of different wood materials as well as the detection of foreign objects (such as rocks) amidst wood chips is possible, as well. The line-scanning spectral imaging system utilized in this study requires that the sample be moved at a steady speed in front of the camera during the measurement. Hence, the NIR-CI measurement is naturally suitable for conveyor belt applications which may be encountered in the sample transportation at a biomass power plant.

Even though the NIR-CI measurement sees only the outermost surface layers of the sample, large sample areas may be measured very quickly with it which increases the representativeness of the measurement. In the current application, the measurement of the area of 30×9.6 cm^2 took 10 seconds. With fiber-optics, the NIR spectral camera may be transformed into a multichannel spectrometer which facilitates the measurement to be conducted simultaneously at several locations (possible dozens or hundreds of metres apart from each other). However, a single channel of the multichannel NIR system collects the spectral data from a very small region (e.g., diameter of 5 mm) making the measurement less representative than in line-scanning spectral imaging.

Several challenges involved with the NIR measurement were identified, as well. They must be addressed individually in each measurement application. First, the chemical and physical differences between different tree species and wood parts will most likely make the use of a single moisture calibration model impossible. Rather, it is likely that the NIR-CI system must first identify the identity of each particle in its field-of-view and then choose a separate calibration model to be used with each encountered particle type. However, in the field of chemometrics and spectroscopic data analysis, there are methods to transform the spectral data such that the differences in the NIR spectra of different wood materials are eliminated, after which the use of a single calibration model for several wood types may be possible. In any case, the heterogeneity of the wood chips must be addressed somehow in the calibration phase. The optimization of the calibration method requires both vast amount of laboratory work – such that a statistically representative calibration data set (comprising NIR spectra and the corresponding reference moisture values from loss-on-drying) is obtained – and experimentation with different data analysis methods.

Another challenge with the NIR analysis of wood chips is the sensitivity of the molecular vibrational states to temperature. For example, the NIR absorption bands of water move towards smaller wavelengths when the temperature is increased. It may be that a single calibration model may not be applicable at the ambient temperatures of +5 °C and +30 °C. Moreover, the characteristic

NIR absorption spectra of liquid water and solid ice are very different from each other, making the moisture analysis of sub-zero samples difficult in the winter. The temperature effect may possibly be addressed through data analysis procedures via eliminating the temperature effects with spectral pre-processing or via constructing a tuneable calibration model, whose parameters are adjusted according to an external temperature measurement. If it seems that the elimination of the temperature effect is impossible, and that the temperature variations degrade the performance of the moisture measurement, the final option is to let the temperature of the sample stabilize, e.g., to +25 °C, prior to measurement. Evidently, the elimination of the temperature effect in wood chip NIR moisture measurements requires vast amount of experimentation with realistic samples and measurement settings.

In the course of the current study, it was demonstrated that the NIR-CI measurement has an effect on the moisture level of the sample. The high-intensity halogen illumination (which is required to provide enough back-scattered photons) heats the sample up, and thus causes evaporation of moisture. This effect was confirmed via duplicate measurements on each sample. As expected, the absorption bands of moisture were slightly shifted towards smaller wavelengths as a result of the increase in sample temperature. Moreover, the predicted moisture level was always slightly lower in the second measurement which was performed immediately after the first. The exposure of the sample to the halogen lamp illumination for the period of 10–20 seconds is thus sufficient to cause changes in the temperature and moisture level of the sample. Since the mass of the samples were not measured during this project, it is not certain whether the decrease in the predicted moisture level is caused by a real evaporation of moisture, or by the shift in the NIR band location (which has an effect on the WCR value, as well). Most likely both phenomena played a part in the results.

The effect of evaporation may possibly be minimized with specifically designed hardware. First, the illuminated area should be minimized. Since the line-scanning NIR spectral camera sees a narrow line on the sample surface at a time, it suffices to illuminate this line while keeping the remaining sample unexposed to the light. This reduces the time the sample spends under halogen lamp illumination. Second, water has strong absorption bands also in the mid-infrared spectral range (wavelengths between 3–5 μm), and since the emission spectrum of a halogen lamp contains these frequencies, as well, the absorption of mid-infrared radiation is a major cause for the heating of the sample in the current application. However, since this spectral range is not utilized by the NIR-CI measurement, the heating of the sample could possibly be reduced via attenuating the intensity of the radiation incident on the sample surface at the mid-infrared wavelengths. A high-pass filter plate which would pass the high frequencies (i.e. shorter wavelengths in the range 900–2500 nm) and block the low frequencies (long mid- infrared wavelengths between 3–5 μm) could possibly be placed between the halogen lamps and the sample to achieve this (see (Thygesen et al. 2000a) for an application).

Finally, NIR instruments tend to be more expensive than conventional machine vision camera systems operating at visible wavelengths. The price of the line-scanning spectral imaging system utilized in this system is between 80–100 K€. If the wavelength range can be reduced to 900–1700 nm, a less expensive NIR detector (InGaAs) becomes feasible, and the price of the system cost drops to 50–60 K€. Despite the high price, the acquisition of an NIR system may be appealing, if moisture analysis costs may be significantly reduced via shortened analysis times (~10 seconds per sample), and reductions in sample storage requirements. The utilization of a multipoint NIR spectrometer and fiber-optic probe heads may be a more cost-effective solution due to the possibility to measure moisture levels simultaneously at several locations.

Table 24. Opportunities and challenges of NIR-CI measurement in the analysis of wood chips.

Opportunities	Challenges
Sensitivity to moisture	Chemical and physical differences between different parts of wood
Chemical sensitivity towards foreign materials (e.g. rocks	Only surface of samples is measured
Spectral imaging makes fast measurement of large surface area possible	Temperature dependence
Line-scanning spectral imaging is naturally suitable for conveyor belt applications	Invasive measurement – high-intensity illumination evaporates moisture
Possibility for multipoint measurement	Expensive compared to visible wavelength cameras

14 Discussion

As explained in previous chapters, distinguishing wood chip types, determining moisture differences and detecting impurities or determining the particle size of wood chips with machine vision technology using visible light is based on colour tone value differentiation. Reliable and/or exact determination can only be done for wood chips that fall into 'standard' wood chip type categories and either the moisture or wood species should be known beforehand. In other words, wood chip samples should not contain deviating factors such as staining of bark or mixed wood species. On the other hand, if wood chip types are to be distinguished with RGB colour cameras, samples should represent the same moisture levels.

In practice, however, different colour tones are affected by several ambient factors like lighting, moisture content of chips, geometry and camera settings (lens opening, exposure time, etc.). When creating identification colour tone functions, these factors should be known and they should be kept as consistent as possible. This makes both the recognition of wood chips and determining of moisture very challenging as far as practical application are concerned.

RGB photographs seemed to cope much better with recognizing shapes and possible impurities but again colour tones are the crucial factor in any analysis. If odd particles are the same colour as wood chips, they are very difficult to detect with this technology. On the other hand, it seems likely that wood chips could be categorized by size using algorithms drawn from RGB photographs.

Measuring wood chip loads with a time-of-flight (TOF) camera rendered the most promising results. Volumes measured with this camera corresponded quite well with manually measured volume values. An average error in these initial tests was about 10%. It should be noticed, however, that a TOF camera is very sensitive to direct sunlight, and therefore it can be concluded that if wood chip loads are photographed with this camera, it should be take place indoors or where illumination is stable.

All in all, both tested machine vision solutions using visible light seemed to have more challenges that direct applications for wood chip analysis and monitoring. In addition to challenges mentioned above, these cameras cannot take reliable pictures of moving wood chips, and therefore they are not suitable for on-line measuring. However, with accepting certain limitations, they could be considered for determining wood chip types and estimating wood chip volumes.

Compared to visible light technology, near infrared (NIR) spectroscopy proved to be much more accurate in determining moisture and detecting foreign materials among wood chips. Advantages and possibilities to use NIR were summarized in the previous chapter. The most obvious strengths of NIR spectroscopy are its ability to accurately measure moisture and detect foreign particles in an on-line setting. Therefore, near infrared cameras could be used at a power plant or fuel wood terminal where wood chips are moved with a conveyer. How to use this technology in winter and in changing outdoor conditions is still uncertain and requires more studies. Analysing moisture of wood chips in a laboratory environment could be done accurately with NIR, however. With tested algorithms, moisture results could be obtained immediately, and thus NIR spectroscopy might be an alternative for measuring moisture with more traditional methods such as oven drying.

References

Allen, R.G., Pereira, L.S., Raes, D. & Smith, M. Crop evapotranspiration – Guidelines for computing crop water requirements. Irrigation and drainage paper 56. Rome: UN-FAO. 1998. 300 p.

Antti, H., Sjöström, M. & Wallbäcks. L. Multivariate calibration Models using NIR spectroscopy on pulp and paper industrial applications. Journal of Chemometrics. (10). 1996. 12 p.

Arlinger, J. Nordström, M. Möller, J.J. StanForD 2010 Modern communication with forest machines. Arbetsrapport 785. Skogforsk. Uppsala. 2012. 22 pp.

Austrian Standards, [online] search: standards for solid biofuels. https://www.austrian-standards.at/home/. 2014.

Berntsson, O., Burger, T, Folestad, S., Danielsson, L.-G., Kuhn, J. & Fricke, J. Effective sample size in diffuse reflectance near-IR spectrometry; Analytical Chemistry. 71. 1999. 6 p.

Elber, U. Feuchtegehalt-Änderungen des Waldfrischholzes bei Lagerung im Wald. Bundesamt für Energie BFE. 2007. 31 p.

Erber, G., Kanzian, C. & Stampfer, K. Predicting moisture content in a pine log wood pile for energy purposes. Silva Fennica 46 (4). 14 p.

Filbakk, T., Hoibo, O. & Nurmi, J. Modelling natural drying efficiency in covered and uncovered piles of broadleaf trees for energy use. Biomass and Bioenergy 35 (1). 2011a. 10 p.

Filbakk, T., Hoibo, O., Dibdiakova, J. & Nurmi, J. Modelling moisture content and dry matter loss during storage of logging residues for energy. Scandinavian Journal of Forest Research Vol. 26. 2011b. 11 p.

Gautam, S., Pulkki, R., Shahi, C. & Leitch, M. Fuel quality changes in full tree logging residue during storage in roadside slash piles in Northwestern Ontario. Biomass and Bioenergy Vol 42. 2012. 8 p.

Golser, M., Pichler, W. & Hader, F. Energieholztrocknung. Holzforschung Austria. 2005. 138 p. Hailwood, A.J. & Horrobin, S.. Absorption of water by polymers: Analysis in terms of a simple model.Trans. Faraday Soc. 42B. 1946. 18p.

Hakkila, P. Forest seasoning of wood intended for fuel chips. Communicationes Instituti Forestalis Finniae 54.4. Helsinki. 82 p.

Hartmann, H. & Kaltschmitt, M. Energie aus Biomasse: Grundlagen. Techniken und Verfahren. Springer Verlag. Berlin–Heidelberg–New York. 2001. 770 p.

Höldrich, A., Hartmann, H., Decker, T., Reisinger K., Sommer, W., Schardt, M., Wittkopf, S. & Ohrner, G. Rationelle Scheitholzbereitstellungsverfahren. Berichte aus dem TFZ 11. Technologie und Förderzentrum im Kompetenzzentrum für Nachwachsende Rohstoffe. 2006. 279 p.

Jirjis, R. Storage and drying of fuel wood. Biomass and Bioenergy Vol. 9. 1995. 5 p.

Jiris, R., Lehtikangas, P. Fuel quality and dry matter loss during storage of logging residues in a stack. Swedish University of Agricultural Sciences. Department of Forest Products. Report 236. 1993.

Kofman, P.D. & Kent, T. Long term storage and seasoning of conifer energy wood. Coford Connects Harvesting/Transportation 20. 2009. 4 p.

Kröll, K. Trocknungstechnik: Trockner und Trocknungsverfahren. Springer Verlag. Berlin–Heidelberg–New York. 1978. 654 p.

Lin, J. & Brown, C.W. Near-IR fiber-optic temperature sensor. Applied Spectroscopy. 47. (1). 1993. 7p.

McMinn, J.W. Transpirational drying of red oaks, sweetgum and yellow poplar in the upper Piedmont of Georgia. Forest Products Journal 36(3). 1986. 8p.

Möller, J., Hannrup, B., Larsson, W., Arlinger, J., Barth, A. & Wilhelmsson, L. Forest fuel. How big is its potential volume? The harvester has the answer. (Hur mycket skogsbränsle blir det? Skördaren ger svaret.) Resultat 15. Skogforsk. Uppsala. 2009. 4 p. (In Swedish with English summary)

Neußer, H., Krames, U. & Streba, H. Ausarbeitung einer Methode zur Holzübernahme nach Gewicht. Österreichisches Holzforschungsinstitut. 1981. 22 p.

Nieuwmeyer, F.J.S., Damen, M., Gerich, A., Rusmini, F., Van der Voort Maarschalk, K. & Vromans, H. Granule characterization during fluid bed drying by development of a near infrared method to determine water content and median granule size. Pharmaceutical Research. 24 (10). 2007. 8p.

Nordfjell, T. & Liss, J.-E. Compressing and Drying of Bunched Trees from a Commercial Thinning. Scandinavian Journal of Forest Research Vol. 15. 2000. 7 p.

Nurmi, J. & Hillebrand, K. The characteristics of whole-tree fuel stocks from silvicultural cleanings and thinnings. Biomass and Bioenergy 31 (6). 2007. 12 p.

Nurmi, J. & Lehtimäki, J. Debarking and drying of downy birch (Betula pubescence) and Scots pine (Pinus sylvestris) fuelwood in conjunction with multi-tree harvesting. Biomass and Bioenergy 35 (8). 2010 . 7 p.

Nurmi, J. Heating values of the above ground biomass of small-sized trees. Acta Forestalia Fennica Vol. 236. 1993. 19 p.

–, The effect of whole-tree storage on the fuelwood properties of short-rotation salix crops. Biomass and Bioenergy Vol. 8. 1995. 5 p.

–, The storage of logging residue for fuel. Biomass and Bioenergy Vol. 17. 1999. 7 p. Paaso, J. Moisture Depth Profiling in Paper Using Near-Infrared Spectroscopy. PhD Thesis. VTT Publications 664. 2007.

Pari, L., Civitarese, V., del Giudice, A., Assirelli, A., Spinelli, R. & Santangelo, E. Influence of chipping device and storage method on the quality of SRC poplar biomass. Biomass and Bioenergy Vol. 51. 2013. 8 p.

Persson, E., Persson, T. & Wilhelmsson, L. Flexible freshness criteria for pulpwood - tools to utilize the variation in drying rate of roundwood. Arbetsrapport 537 “Raw Material Utilization”. Proceedings from 2nd Forest Engineering Conference. Skogforsk. Uppsala. 2003. 10p.

Petterson, M. & Nordfjell, T. Fuel quality changes during seasonal storage of compacted logging residues and young trees. Biomass and Bioenergy 31 (11/12) 2007. 11

Röser, D., Erkkilä, A., Mola-Yudego, B., Sikanen, L., Prinz, R., Heikkinen, A., Kaipainen, H., Oravainen, H., Hillebrand, K., Emer, B. & Väätäinen, K. 2010. Natural drying methods to promote fuel quality enhancement of small energywood stems. Working papers of the Finnish Forest Research Institute 186. 2010. 60 p.

Siesler, H.W., Ozaki, Y., Kawata, S. & Heise, H.M. Near-infrared spectroscopy: principles, instruments, applications. Wiley. 2002.

Simpson, W.T. Equilibrium moisture content of wood in outdoor locations in the United States and Worldwide. United States Department of Agriculture. Forest service. Forest Products Laboratory. Research note FPL-RN-0268. 1998. 11 p.

Steger, C., Ulrich, M. & Wiedemann, C. Machine vision algorithms and applications. Wilet-VCH. Weinheim. ISBN: 978-3-527-40734-7. 2007.

Stokes, B.J., Watson, W.F., Miller, D.E. Transpirational drying of energywood. ASAE paper No. 87–1530. St. Joseph. MI: American Society of Agricultural Engineers. 1987. 13 p.

Suadicani, K. & Gamborg, C. Fuel quality of whole-tree chips from freshly felled and summer dried Norway spruce on a poor sandy soil and a rich loamy soil. Biomass and Bioenergy Vol. 17. 1999. 10 p.

Tåg, C.-M., Toiviainen, M., Juuti, M. & Gane, P.A.C. Dynamic analysis of temporal moisture profiles in heatset printing studied with near-infrared spectroscopy. Meas. Sci. Technol. (21). 2010.

Tåg, C.-M. Liquid transportation and distribution during (re)wetting: impact on coated papers in printing; PhD Thesis. Åbo Akademi University. 2013.

Thygesen, L.G. & Lundquist, S.P. NIR measurement of moisture content in wood under unstable temperature conditions. Part 1. Thermal effects in near infrared spectra of wood. Journal of Near Infrared Spectrosc. (8). 2000a. 7 p.

Thygesen, L.G. & Lundquist, S.P. NIR measurement of moisture content in wood under unstable temperature conditions. Part 2. Handling temperature fluctuations. Journal of Near Infrared Spectroscopy. (8). 2000b. 9 p.

Toiviainen, M., Kurki, L., Finta, C., Kögler, M., Kaarre, M., Juuti, M. Final report for a contract research project PROSPEC (Confidential). VTT. 2013.

Wilhelmsson, L., Persson, E. & Persson, T. Predicting the drying rate in harvested roundwood. (Prognoser för virkets uttorkning efter avverkning). Resultat 11. Skogforsk. Uppsala. 2005. 4p. (In Swedish with English Summary).

Workman, J.A review of process near infrared spectroscopy: 1980–1994. Journal of Near Infrared Spectroscopy. (1). 1993. 2.